VĚDECKÉ SPISY VYSOKÉHO UČENÍ TECHNICKÉHO V BRNĚ
Edice Habilitační a inaugurační spisy, sv. 511
ISSN 1213-418X

Václav Veselý

THE ROLE OF PROCESS ZONE IN QUASI-BRITTLE FRACTURE

BRNO UNIVERSITY OF TECHNOLOGY
Faculty of Civil Engineering
Institute of Structural Mechanicss

Ing. Václav Veselý, Ph.D.

THE ROLE OF PROCESS ZONE IN QUASI-BRITTLE FRACTURE

ROLE PROCESNÍ ZÓNY
PŘI KVAZIKŘEHKÉM LOMU

Short version of Habilitation thesis
Constructions and Traffic Structures

VUTIUM

BRNO 2015

KEYWORDS

quasi-brittle fracture, fracture process zone, energy dissipation, work of fracture, fracture energy, effective crack model, cohesive crack model, failure criterion, fracture test, notched specimen, wedge splitting, bending, splitting/bending geometry, constraint, near-crack tip fields, Williams series, higher-order terms, stress field approximation, fnite element analysis, Java application

KLÍČOVÁ SLOVA

kvazikřehký lom, lomová procesní zóna, disipace energie, lomová práce, lomová energie, model efektivní trhliny, model kohezivní trhliny, podmínka porušení, lomový test, těleso se zářezem, štípání klínem, ohyb, štípací/ohybový test, constraint, pole napětí u čela trhliny, Williamsova řada, členy vyšších řádů, aproximace pole napětí, metoda konečných prvků, Java aplikace

The full version of the thesis is deposited in the archive of the Study division of Dean‘s office of Faculty of Civil Engineering at Brno University of Technology

ISBN 978-80-214-5255-8
ISSN 1213-418X

CONTENTS

1 INTRODUCTORY REMARKS

The phenomenon of fracture of solids seems to be deeply understood in individual branches of mechanics of failure, especially from the point of view of the technical disciplines dealing with prediction and assessment of the material behaviour. Technically, it is usually classified as the brittle, the elastic-plastic or the quasi-brittle case (see [34, 6], sketched in Fig. 1). However, problems often arise when approaches proven as valid in one branch of the failure description theory are applied elsewhere. For example, the tools of the linear elastic fracture mechanics (even in the two-parameter expression, e.g. [2]) predict generally wrong failure response in the field of elastic-plastic or quasi-brittle fracture. Likewise, the strength theory (ignoring a stress concentration at the discontinuity tips) and also ductile fracture models are not suitable for failure cases with a rather sudden and massive energy release (typical for brittle fracture and quasi-brittle cases with small material characteristic length).

The problem usually results from inadequate simplifications being considered in the particular discipline (of course, making the assessment within the appropriate field clear and often very elegant). These simplifications usually discredit even the proven and well established models for their application beyond the range of their validity (or near its bounds – the transition area between two neighbouring classes, see Fig. 1).

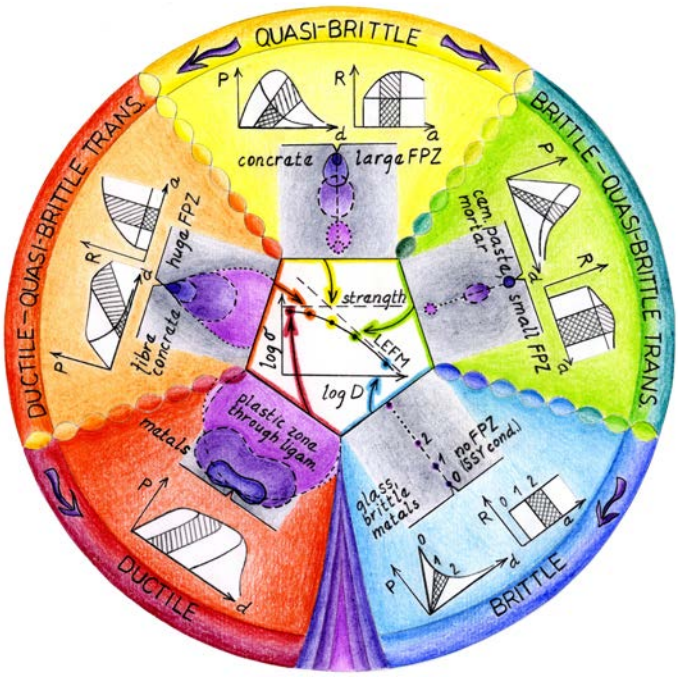

Fig. 1: Sketch of classification of failure of materials, description of their fracture response and the link to scaling law interpreted as a mandala, © Dita Vořechovská, Václav Veselý, 2015

Unified theory (if at all possible) is missing; general enough, based on sound physical cornerstones, but still relatively easily employable for material scientists and engineers. Why is it needed? Since many both natural and man-designed materials (for which ideal prototypes can be found again in the Nature) behave in a manner that combines the superb properties of materials from different classes. Various composite materials with fine-tuned properties of either the matrix and/or the fibres/aggregates (in technics and geonics) and biological tissues originated from both fauna and flora (apart from technics also in bionics and medicine) can be mentioned as examples. These lay typically far away from the cases (see again Fig. 1) for which the traditional theories are valid.

From this perspective, the quasi-brittle fracture may be viewed as a 'superset' to the ductile and the brittle case as it is characterized by an amalgamation of both principal mechanisms of energy dissipation, i.e.

i) the one taking place in the volume of the nonlinear zone (plasticity theory) evolving at the discontinuity tip and releasing the energy spatially over the nonlinear zone via various damage mechanism and
ii) the one taking place at the crack tip and releasing the energy via creation of new crack surfaces (fracture mechanics).

The idea is attempted to be expressed through the 'mandala' in Fig. 1 and forms the

leitmotiv of the present thesis. Therefore, the quasi-brittle fracture behaviour is studied here from the very fundamentals.

Reinforced concrete structures are among the most frequent application of the man-made quasi-brittle material, the cement-based composite – concrete. The failure of these structures is associated with crack initiation and propagation. Thus, fracture-mechanics principles should be employed within the design and assessment of such structures. Many phenomena from the field of damage and failure of silicate-based quasi-brittle materials utilized in the building industry are already well understood, and this has yielded recommendations proposed in design codes (ACI standards, JCI standards, FIB model code etc.) and other relevant documents (e.g. RILEM recommendations). However, some phenomena, which still may be regarded as fundamental, haven't been adequately resolved and explained yet and are still the subjects of scientific research.

One such phenomenon that is worth deeper analysis is the energy dissipation during the tensile failure (fracture) of quasi-brittle materials. Particularly, the description of this phenomenon from the perspective of characterization of the affected material by means of a unique set of parameters is still not clear. These parameters should serve both as characteristics for the classification of the material (describing its resistance to the failure propagation) as well as inputs into adequate material models for numerical simulations of structural behaviour. As such, these parameters must be the true material parameters that don't depend on the size and shape of the specimen(s) on which they are determined as well as on the test set-up and other test/laboratory conditions.

The present thesis is aimed at particularities of the mentioned effect of the size, geometry and boundaries of test specimen on determined values of fracture parameters. As is indicated in the title of this thesis, it is acquired through investigation of the role of fracture process zone (FPZ) in the quasi-brittle fracture phenomenon.

Several chapters are omitted in this shortened version of the thesis. For the detailed 'State-of-the-Art' section and the 'Theoretical background' part introducing methods employed in the conducted analyses see the full version of the thesis. In addition, only some examples were selected from the 'Verification' and 'Validation' parts.

2 MOTIVATION AND OBJECTIVES

The purpose of the presented research is the determination of parameters for fracture models describing the softening nature of the quasi-brittle response of civil engineering structures made of such materials. Particular attention is paid to silicate-based, mainly cementitious composites, however, materials/structures behaving in quasi-brittle manner are very common also in other fields of engineering, science and even nature.

Fracture tests represent the most convenient way of gaining relevant information on the tensile failure behaviour of the studied materials. A number of issues related to the intrinsic relevance of the information obtained from laboratory experiments have been intensively researched and reported in the literature for what is already more than thirty years. From these issues the effect of specimen size, shape and boundary conditions on the determined values of fracture characteristics (a topic on which a general consensus between interested researchers has not yet been reached completely) is of particular relevance here.

An approach incorporating the parameters of the zone of material failure developing at the propagating macroscopic crack tip has been proposed by the author of this thesis with his closest collaborators recently. The development of this approach is motivated by capturing

of the above-mentioned effects in order to provide values of the fracture-mechanical parameters of the tested material independent of these effects. This methodology works with the reconstruction of the current size and shape of the FPZ (and also the intensity of the cohesive behaviour over the FPZ volume) to which the amount of energy dissipated during the current step of fracture process should be related. The development of the methodology is in a stage of testing, verification by numerical simulations and experimental validation at present.

The importance of the research covered in this work arises from the unresolved problems within the topics which are described in detail in the 'Introductory remarks' and the 'State-of-the Art' sections of the full version of the thesis. The gained solutions of conducted studies should yield a possibility to describe the phenomenon of nonlinear fracture of structural/natural materials behaving in quasi-brittle manner by unambiguous fracture-mechanical parameter (most probably set of parameters) which can be regarded as intrinsic material property independent of the size/shape/boundary of the specimen/structure. This is expected to significantly contribute:

i) to effectiveness and safety of utilization of the non-linear fracture mechanics tools in engineering and science within the analyses, design and assessment of man-made structures or natural entities,
ii) to constitution of a reasonable classification of nonlinearly failing materials according to their fracture behaviour.

Primary goals of the research presented in this thesis feature:

1. Refining and better specification (revision, improvement) of the procedures by which the fracture-mechanical characteristics of quasi-brittle materials are determined, especially those concerning the energy dissipation – fracture energy, energy dissipation density within FPZ or similar.
2. Implementation of the said procedures (resulting in a Java application in this case), its formal description, and illustration of its functioning in the context of both real and simulated fractures of specimens in various configurations.
3. Proper testing, verification and validation of the adopted methodology.
4. Fixing of possible problematic issues and reformulation relevant parts of the procedure.

The objectives 2 and 3 shall be acquired via conduction of a coherent research of nonlinear fracture behaviour of silicate-based composites, and that in a broader sense from the perspective of the material composition/inner structure and from that resulting fracture behaviour type (which can be characterized by the extent of the nonlinear zone at the propagating fracture front described in a simplified way by e.g. the characteristic length value). Within this research, several materials differing in its characteristic length as well as different fracture test geometries on specimens with varying shape, size, and notch length shall be investigated.

Experimental evidence for these objectives is sought in literature, however, also own experimental programs will be conducted for which specific test geometries are going to be used. Thus, considerable attention is paid to investigation of possibilities and limits of a newly proposed configurations of fracture test based on the combination of boundary conditions of TPB/FPB and the WS geometry, and modified CT test, where the tensile load eccentricity varies. It is expected that tests performed in these configurations, enabling a wide range of variants of the stress distribution in the test specimen leading to variations of the size and shape of developed FPZ, will bring new insight into problem of size/geometry/boundary effects on fracture parameters and strengths of the materials. A thought-out experimental campaigns are preceded/accompanied by detailed numerical analyses. The obtained experimental/simulation data are then evaluated using the developed technique and compared to already established advanced models relevant the investigated phenomena.

3 HYPOTHESIS

The author with collective of his close collaborators is primarily focused on the estimation of the size, shape and other relevant properties of the zone with nonlinear material behaviour evolving at the tip of a propagating crack in composite materials with disordered internal structure, i.e. those with a quasi-brittle nature exhibiting strain softening, in particular cementitious composites. Fracture propagation in mode I is considered. The characteristics of the fracture process zone are intended to be utilized within methods for the evaluation of fracture mechanical parameters in order to diminish the effects of the test specimen size, geometry and free boundaries on the values gained for such parameters using established techniques of the test records evaluation. The main focus is on fracture energy here. This parameter, serving as the main input in the cohesive-crack based models for simulation of failure in softening materials, suffers from the above-mentioned effects when it is determined from records of tests on laboratory-sized specimens via the work of fracture method [32]. Similar situation exists within the models of equivalent elastic crack and the related $\mathcal{R}$-curve description.

This topic has been rather intensively researched in connection to quasi-brittle fracture in the last decades, as is evident from the 'State-of-the-Art' section covered in the full version of the habilitation thesis. Models containing remedies for that disadvantage have been published in recent years, e.g. [5, 9, 11, 19, 23, 31]; however, the particular parameters of the FPZ are considered within these models only in a schematic simplified manner and the proofs of these models are available only for test configurations with (moderate and) high level of crack tip constraint. According to opinion of the author, a more general validation should be conducted.

3.1 Work of fracture divided into two parts

With regard to this problem, a hypothesis has been introduced by the author and his coworkers in [53, 52, 54] proposing the capturing of the size/shape/boundary effect on the fracture-mechanical parameters of the aforementioned materials through relating the energy dissipated for the fracture process (the work of fracture) not only to the (projection of the) created fracture surface (as it is treated within the work-of-fracture method [32]) but also to the volume of the FPZ. Graphical interpretation of the presumption of the hypothesis is sketched in Fig. 2.

Thus, an increment of the energy dissipated at one time step of a quasi-brittle fracture process $\mathrm{d}\mathcal{W}_\mathrm{f}$ can be divided into a part released for the creation of new fracture surfaces, like the Irwin-Griffith crack, $\mathrm{d}\mathcal{W}_\mathrm{f,s}$ (subscript 's' denotes 'surface') and a part dissipated in the volume of the current fracture process zone $\mathrm{d}\mathcal{W}_\mathrm{f,z}$ (with the subscript 'z' denoting 'zone')

$$\mathrm{d}\mathcal{W}_\mathrm{f} = \mathrm{d}\mathcal{W}_\mathrm{f,s} + \mathrm{d}\mathcal{W}_\mathrm{f,z} \ . \tag{1}$$

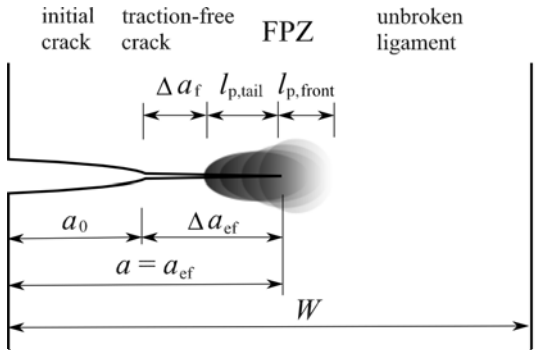

Fig. 2: Schema of the FPZ existing at the tip of propagating crack in quasi-brittle material

The part released for the creation of the new fracture surfaces can be specified by the crack area (namely its projection to the crack plane) as the natural descriptor of this entity resulting from that physical phenomenon. This leads to the well known definition of the fracture resistance $\mathcal{R}$ (or toughness $\mathcal{G}_\mathrm{c}$) [Jm^{-2}] as it is defined for the case of ideally brittle materials

$$\mathcal{G}_\mathrm{c} = \frac{1}{B}\frac{\partial \mathcal{W}_\mathrm{f}}{\partial a_\mathrm{ef}} \ , \tag{2}$$

where a_{ef} is the effective crack length and B the specimen breadth.

If the value of the other part $\mathrm{d}\mathcal{W}_{\mathrm{f,z}}$ is not negligible and yet is ignored in such an evaluation, i.e. the whole dissipated energy $\mathrm{d}\mathcal{W}_{\mathrm{f}}$ is assigned to be released for the enlargement of the crack surface, the size/shape/boundary effect is present to certain extent in the investigated fracture behaviour. Its significance then depends on the mutual relation of $\mathrm{d}\mathcal{W}_{\mathrm{f,z}}$ and $\mathrm{d}\mathcal{W}_{\mathrm{f}}$; the larger is the $\mathrm{d}\mathcal{W}_{\mathrm{f,z}}/\mathrm{d}\mathcal{W}_{\mathrm{f}}$ ratio the more noticeable is the nonlinearity connected to the fracture process resulting in size/shape/boundary effect expression. On the other hand, if $\mathrm{d}\mathcal{W}_{\mathrm{f,z}}$ tends to zero, the classical fracture mechanics functions normally.

The part of the energy dissipated in the volume of the fracture process zone $\mathrm{d}\mathcal{W}_{\mathrm{f,z}}$ shall also be specified in some manner by the characteristics of the region where the failure process takes place to obtain a parameter describing the volumetric energy dissipation due to softening, referred to as the energy dissipation density $\mathcal{H}_{\mathrm{f}}$ [Jm^{-3}] in this work. The most straightforward method of doing this would be to relate the energy directly to the FPZ volume, as was done in previous studies [53, 55], i.e.

$$\mathcal{H}_{\mathrm{f}} = \frac{\mathrm{d}\mathcal{W}_{\mathrm{f,z}}}{\mathrm{d}V_{\mathrm{z}}} \ , \tag{3}$$

where V_{z} is the volume of the cumulative damage zone (CDZ). The CDZ is an envelope of FPZ's for all stages of fracture process from its beginning to the current stage. In this work, the CDZ (and FPZ) volume is considered simply as the multiplication of the CDZ (FPZ) area Ω_{CDZ} (Ω_{FPZ}) and the specimen breadth B. Incorporation of models capturing the change of the CDZ (FPZ) extent along the specimen breadth, e.g. that in [10] or others, is planned in future research.

However, this assumption appeared to be too strong, as a substantial non-uniformity of the energy dissipation distribution has become obvious[1]. Nevertheless, even this assumption is much closer to reality than that of the work of fracture method where the energy dissipated for quasi-brittle fracture is averaged for the whole created crack area, which means that the method assumes just an uniform energy dissipation along the propagating crack and ignores the existence of FPZ (which, furthermore, changes its extent during that process).

In the present research of the author, the parameter(s) describing the volumetric dissipation of energy is (are) sought with respect to the proper distribution function. Recently, the described approach is being tested by the author and his collaborators on data of several experimental campaigns, e.g. that published in [30, 39, 40, 18, 42, 15, 16]. In several cases the recorded data are not directly suitable for the intended fracture analysis (usually due to insufficient accuracy of displacement measurements). Thus, accompanying numerical simulations must have been conducted in connection to some of these data (see e.g. [47]). Moreover, own precisely targeted experimental campaigns are under preparation, for details see Sec. 5.

3.2 Uniform amount of energy dissipated for fracture propagation

The next assumption postulated within the hypothesis is that the specific energy needed for both the crack propagation and the FPZ evolution is constant and is regarded as the material property.

Decomposition of the whole work of fracture value $\mathcal{W}_{\mathrm{f}}$ into the two parts is based on the idea that a specific load level is assigned to be the initial load by which the propagation of the effective crack begins. Up to this load, the crack is not propagating, the P–d curve is straight for linear elastic materials, see Fig. 3 top. The energy release rate corresponding to this

[1]This fact has been proven also experimentally [30, 39, 16] and via numerical simulations [14, 12, 16].

load is then kept constant for the further effective crack propagation (see the red descending branch). Thus, the area under the load–displacement curve, i.e. the energy dissipated for the quasi-brittle fracture $\mathcal{W}_{\mathrm{f}}$, is divided into two regions: The part assigned to the stress-free (effective) crack advance (corresponding to 'brittle' fracture) $\mathcal{W}_{\mathrm{f,s}}$ and that corresponding to failure mechanisms taking place in the nonlinear zone $\mathcal{W}_{\mathrm{f,z}}$, which results in incorporation of a certain level of 'quasi-brittleness' to the observed phenomenon.

Both parts of the energy, expressed either in the cumulative form reflecting the averaged energy release from the beginning of the fracture propagation to the current stage (blue hatch) or in the incremental form, reflecting the instantaneous energy release (green hatch), are then related to spatial parameters of the corresponding entities which are the outcomes of the fracture phenomenon within this model, i.e. the crack area and the FPZ volume. Thus, constant $\mathcal{R}$-curve for the effective crack propagation (see Fig. 3 bottom left) and constant $\mathcal{H}$-curve for the FPZ evolution (Fig. 3 bottom right) are sought to characterize this model.

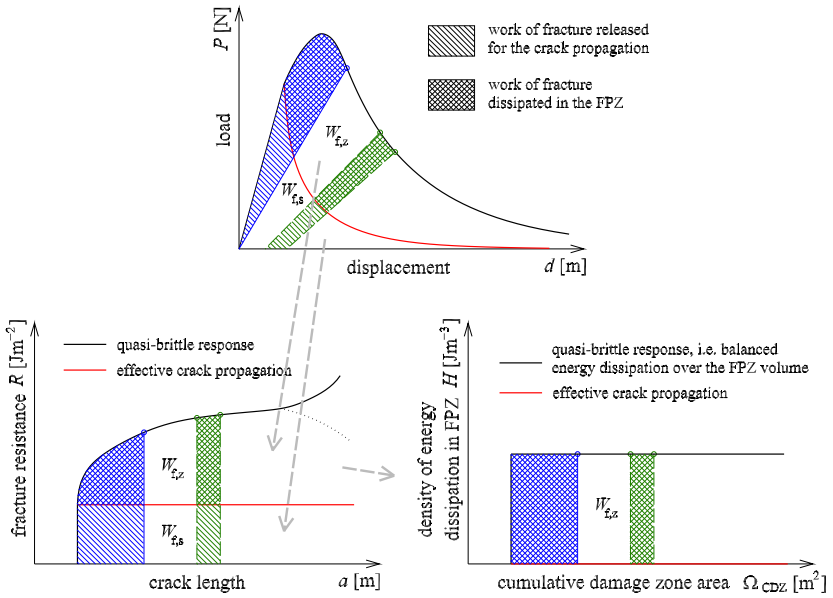

Fig. 3: Representation of the work of fracture portions released for both the crack propagation and the FPZ development in the P–d diagram, $\mathcal{R}$-curve and $\mathcal{H}$-curve

Note that whereas the relation of $\mathcal{W}_{\mathrm{f,s}}$ and a_{ef} is clear, the link between $\mathcal{W}_{\mathrm{f,z}}$ and the FPZ extent is still being researched.

Lines representing current compliances of the tested specimen in the P–d curve in Fig. 3 top don't consistently lead to the origin. It is sketched in this way on purpose: In some cases, mainly for small specimens with large FPZ, a considerable phenomenon manifested as apparent plasticity is often observed in experimental records (see the green unloading compliances), which can be related to a large portion of $\mathcal{W}_{\mathrm{f,z}}$. On the other hand, when the FPZ extent is negligible, the energy dissipates only for fracture and, therefore, unloading compliance lines point to zero.

3.3 Note to origination of the hypothesis

The above-proposed hypothesis, i.e. the idea of splitting the energy dissipated for the fracture in the part for the crack propagation and the FPZ evolution, was inspired by a similar idea published in [34]. The nonlinear fracture is described in that textbook as an amalgamation of the Irwin-Griffith mechanism of energy dissipation, where the energy rate $\mathcal{G}_{\mathrm{c}}$ is released during the creation of two stress-free crack surfaces, and the Dugdale-Barenblatt mechanism of energy dissipation, where the energy rate $\mathcal{G}_{\sigma}$ is consumed for overcoming of the cohesive traction $\sigma(w)$ in order to separate the crack surfaces

$$\mathcal{G}_{\mathrm{q}} = \mathcal{G}_{\mathrm{c}} + \mathcal{G}_{\sigma} \ . \tag{4}$$

If the $\mathcal{G}_\sigma$ term is neglected, the equivalent elastic crack model description applies. On the other hand, when the Irwin-Griffith crack propagation is ignored, the pure cohesive crack approach holds.

The model proposed here utilizes the same idea; however, the phenomenon of energy dissipation is being split in the two parts on the level of the work of fracture (in [J]) calculated directly from the load–displacement curve, as the two amounts of energy released via changes of different entities produced by the fracture phenomenon, i.e. the (effective) crack and the fracture process zone, are specified by descriptors of the measure of these entities, i.e. of the area of the crack and the volume of the FPZ.

Construction of the descending branch corresponding to brittle crack propagation (at constant $\mathcal{G}_c$) is inspired by the Double-K model [31]; within this model the red curve from Fig. 3 would correspond to $K_{c,ini}$. Similar approach as the one sketched in the bottom left graph of Fig. 3 was used in [41]. However, none of these models utilize the real spatial characteristics of the FPZ. From this point of view, the proposed model can be considered as a novel approach.

4 PROPOSED METHODOLOGY – RECONSTRUCTION OF FRACTURE PROCESS (ReFraPro)

The technique is being developed to refine methods for determination of the fracture mechanics parameters of quasi-brittle cementitious materials. It should provide real material parameters describing the tensile failure of such materials, in contrast to the existing methods (e.g. [32, 33]) that suffer from the influence of the test specimen size, geometry or boundary conditions on the determined values of fracture parameters.

4.1 ReFraPro procedure for determination of fracture properties of quasi-brittle materials

Based on the facts presented in Sec. 2 (and mainly the 'State-of-the-Art' section of the full version of the thesis) a hypothesis has been proposed in Sec. 3. It can be condensed to the form of the following paragraph:

> *The determination of the fracture parameters of quasi-brittle materials which are not (or are much less) dependent on the test specimen size, geometry properties and boundary conditions of the test can be achieved via methods for the evaluation of fracture test records that take into account the existence of the FPZ and the energy dissipation within it. Such an approach to the FPZ incorporation has to be specific; in particular, the current size and shape of the nonlinear zone during the fracture process should enter the evaluation procedure. This procedure should also relate a portion of the current amount of energy released at each individual stage of the fracture process (i.e. a portion of the current increment of the work of fracture) to the characteristics of the current FPZ (i.e. its size and shape, and the energy dissipation distribution over it). The second portion of the energy dissipation is linked to some of the characteristics of the propagating (traction-free) crack, i.e. its length or opening.*

This approach converges to brittle fracture with decreasing FPZ size and/or increasing specimen size – the whole energy release is due to crack propagation, because the negligible FPZ extent implies that there is almost no energy dissipation within it. In the opposite direction, the strength theory is met when the FPZ (or asymptotically only its core part with

almost no softening) is spread over the whole specimen cross-section. For illustration of this approach, Fig. 1 can be again reminded.

In this section, the first part of the theory is presented, which is focussed on the estimation of the FPZ extent[2].

The approach is being implemented in a computer application which is designed for the processing of records of fracture tests in order to evaluate the fracture parameters of the material of the tested specimens. This processing is conducted as a reconstruction of the fracture process taking place in the testing device. The name ReFraPro was therefore chosen for the application; it is an acronym for Reconstruction of Fracture Process. The subsequent paragraphs of this section feature a detailed description of the application, which is preceded by brief sketch of the programme architecture. A thorough examination of the implemented approach is illustrated here on an example of numerically simulated fracture test.

4.1.1 Structure of the ReFraPro application – The programme architecture

An object-oriented programming paradigm was used for the creation of an application for the evaluation of quasi-brittle fracture parameters. It was programmed in JAVA [20] programming language. The application is designed to be used for 2D fracture problems in various test configurations. For the present, the application is limited to several mode I fracture geometries, such as the single edge notched beam under three point bending (SEN-TPB) and the wedge splitting test (WST) variants. However, it is expected that extensions for other arbitrary tensile fracture mode configurations or also in-plane mixed-mode ones will be implemented. The object-oriented structure is ideal for this purpose.

The programme architecture was proposed and its structure created by dr. Petr Frantík from the author's institute. The author of this thesis formulated the methodology of the approach implemented into the application and participated on programming of classes implementing the fracture-mechanical models and theories. For detailed description of the object-oriented structure and other relevant programming details see [52]. In that paper, the authors were limited to the description of only the part of the ReFraPro application dealing with the determination of the FPZ extent. Note that the structure of the program also contains other objects dealing with the calculation of the current/cumulative portions of the energy dissipated during fracture (the work of fracture), the relation of these energy amounts to characteristics of the equivalent elastic crack and fracture process zone, the construction of $\mathcal{R}$-curves, etc.

4.1.2 ReFraPro estimation of the nonlinear zone extent

The implemented procedure is described in individual steps here. Selected steps are accompanied by corresponding graphical output from the application illustrating the utilized methods. Relevant parts of a formerly published analysis [51, 52] are shown.

A notched beam of dimensions $L \times W \times B$ equal to $0.48 \times 0.08 \times 0.08$ m with an initial crack (notch) of length $a_0 = 0.008$ m (relative notch length $\alpha_0 = a/W = 0.1$) loaded in three-point bending was chosen as an illustrative example, see Fig. 4 top left. The beam is supposed to be made of concrete with the following fracture-mechanical parameters: tensile strength $f_t = 3.7$ MPa, fracture energy $G_F = 93$ Jm^{-2}, and exhibiting exponential (Hordijk's) softening. The fracture test of the beam was simulated numerically using ATENA software [8]. The recorded load–displacement diagram is plotted in Fig. 4 bottom left, where six stages

[2]Frankly speaking, the whole present work is focussed mainly on this issue. The second part of the hypothesis, i.e. the connection of the FPZ with the energy dissipation within it is only indicated in its basic aspects. This issue is recently under intensive research by the author and his co-workers.

of the fracture process are emphasized, from A to F, corresponding to relative effective crack lengths α equal to 0.15, 0.35, 0.53, 0.7, 0.87, and 0.97, respectively.

1. Inputs to the procedure are entered, such as the specification of the test configuration and specimen dimensions (in this case according to Fig. 4 top left), basic mechanical properties of the tested material (the compressive and tensile strength f_c and f_t, respectively[3]) and the load–displacement diagram (P–d curve, Fig. 4 bottom left). Guess values[4] of parameters of the cohesive crack model, particularly the fracture energy value G_F and the cohesive stress function $\sigma_{coh}(w)$, are entered into the procedure as well.

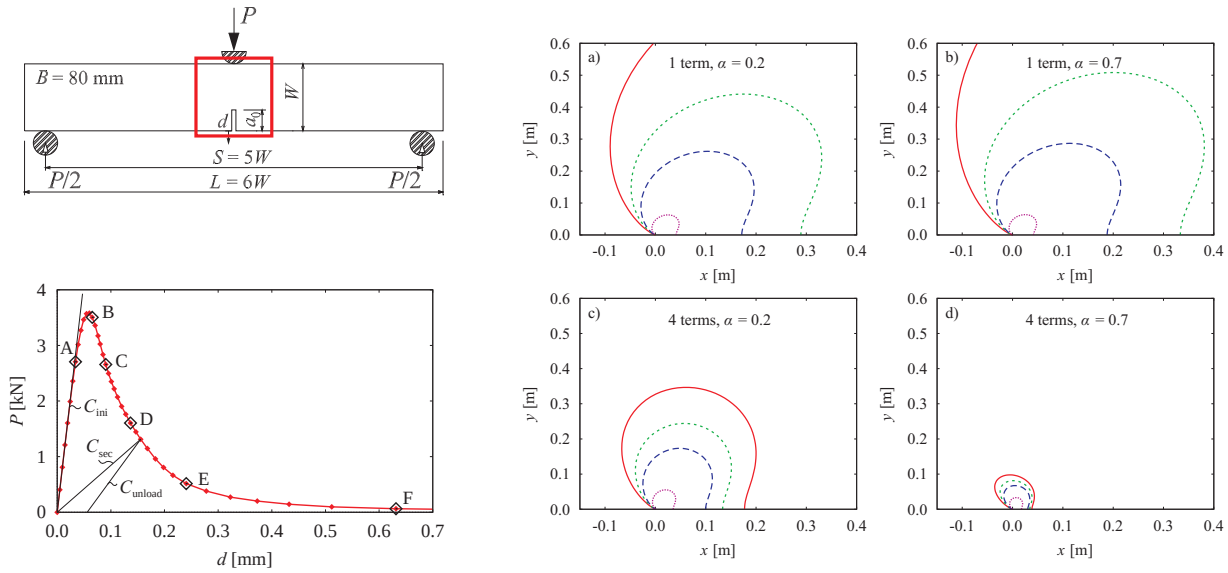

Fig. 4: Left: SEN-TPB testing configuration (top), numerically simulated P–d diagram for the above-described beam including values for six stages of the fracture process (bottom); right: corresponding isolines of the σ_{yy} stress tensor component for the SEN-TPB example for relative crack length $\alpha = 0.2$ (left) and 0.7 (right) for one (top) and four (bottom) terms of the Williams series

2. Subsequently, the P–d diagram is processed to obtain the initial compliance C_{ini} of the tested notched specimen from which Young's modulus E is calculated.
3. For arbitrary stage i of the fracture process, i.e. a point on the P–d curve, the length of the equivalent elastic crack $a_{e,i}$, or the effective crack increment $\Delta a_{e,i}$, is estimated by means of the effective crack model [29]. An iterative scheme is used based on comparison of the initial compliance C_{ini} corresponding to the specimen with a notch (initial crack) with the current compliance corresponding to the specimen with an effective crack of the current length.
4. Similarly to the previous point, for each stage, values of the crack mouth opening displacement ($CMOD$) are calculated from the crack lengths using the LEFM formula appropriate to the investigated test geometry.
5. In the next step, the energetic quantities are calculated such as the cumulative and current work of fracture, the fracture energy, and the $\mathcal{R}$-curve (or K_R-curve) are constructed, etc. Details on these evaluations can be found in [53, 57].

[3]The parameter f_c is necessary when a more complex failure criterion which takes the compressive strength into account is used. In the case of this example the Rankine failure criterion was employed; therefore, f_c is not specified.

[4]These values may be updated via inverse analysis in order to obtain outputs of the procedure corresponding with the inputs.

6. Subsequently, multi-parameter linear elastic fracture mechanics tools are employed. For each stage of the fracture process to which the estimated value of (equivalent elastic) crack length corresponds, the stress field at the crack tip (not necessarily only in its very vicinity) is approximated using the Williams power series [43]. In order to keep the approximation accurate enough even in the more distant surroundings of the crack tip, which is essential for quasi-brittle materials with a large FPZ, the higher order terms of the series are also taken into account.
   Particularly, values of coefficients of terms of the William series A_n are computed for the current relative crack length α and nominal stress σ from dimensionless geometry functions $g_n(\alpha)$. These are typically polynomial functions.
   Subsequently, stress state descriptors are calculated, such as the individual components of the stress tensor σ_{xx}, σ_{yy}, τ_{xy} and its eigenvalues σ_1, σ_2.
   The necessary number of terms N in the Williams series must be chosen with respect to the mutual relation between the FPZ extent and the size/shape of the body (with respect to the distance between the FPZ and the boundaries of the body)[5]. Considering the higher order terms of the expansion enables the capturing of changes in the stress gradient (influencing the size and shape of the FPZ) during the crack propagation. Their importance is depicted in Fig. 4 right, where the σ_{yy} distribution is, due to symmetry, shown for only one half of the specimen. Striking differences can be seen especially for large cracks, which correspond to the high constraint level in the case of the SEN-TPB geometry.
7. Plasticity theory tools are utilized for the determination of the inelastic zone contour. The extent of the zone where the until-now elastic material starts to 'yield', denoted here as Ω_{PZ} (the initials 'PZ' in the subscript stand for Plastic Zone), is determined by comparing the tensile strength f_{t} of the material to proper characteristics of the stress state around the crack tip (some sort of equivalent stress σ_{eq} for cementitious composites, e.g. the Rankine failure criterion, can be employed.)
   Direct evaluation of the radius r and angle θ might not be possible if more than two terms of the Williams series are used (for up to two terms of the series the radius r can be explicitly expressed as a function of the angle θ). To keep the procedure general enough, the calculation of the plastic zone boundary is performed iteratively using Newton's method.
   Fig. 5 left shows a comparison of the plastic zone contours determined by three different yield criteria in which the equivalent stress σ_{eq} ($= \sigma_{yy}$, σ_1 for the Rankine, and σ_{DP} for the Drucker-Prager criterion in the plane stress state, respectively) is given as being equal to tensile strength f_{t}. Four terms of the Williams series were considered. Again, similarly to the above item, the change in the size and shape of the plastic zone contours is clearly visible.
8. The further step in the ReFraPro procedure is the calculation of crack face profiles. For each fracture stage i to which an equivalent elastic crack of length $a_{\mathrm{e},i}$ corresponds, crack opening displacement (COD) values are calculated using appropriate LEFM formulae, for the SEN-TPB geometry e.g. that from [36]. The COD values are computed at locations on the current crack face where the crack tip was located in the previous fracture stages (from $i-1$ to 0).

[5]It is recommended to estimate this by trial-and-error based on convergence saturation of the results from that part of the procedure with increasing N.

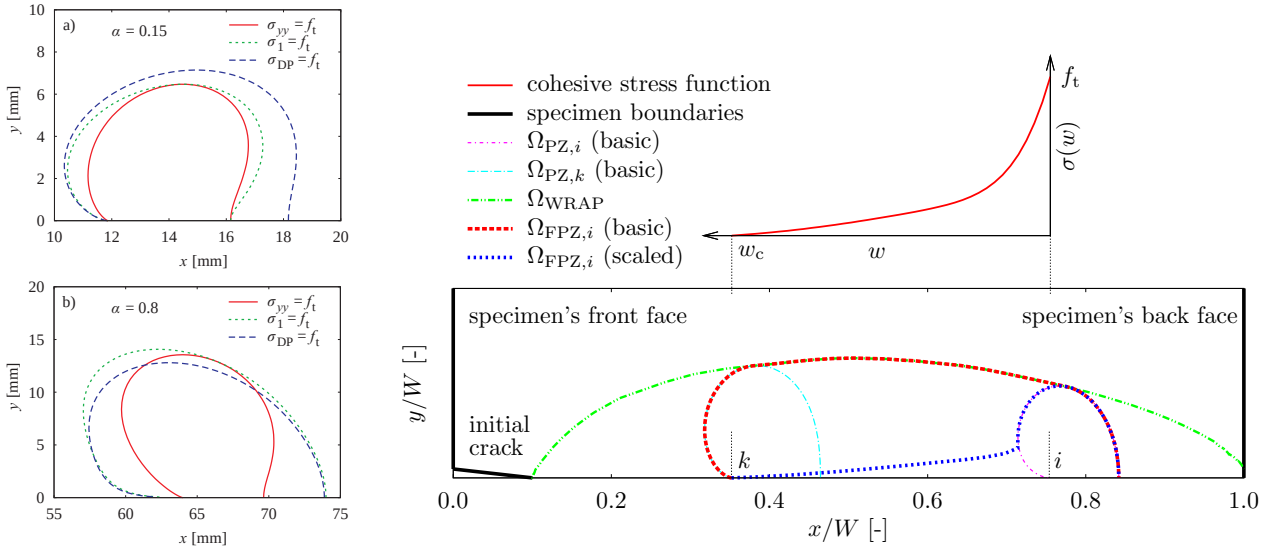

Fig. 5: Left: Depiction of plastic zone contour Ω_{PZ} for σ_{yy}, Rankine and Drucker-Prager failure condition for $\alpha = 0.15$ (a) and 0.8 (b); right: construction of failure zone extents – typical cohesive law for quasi-brittle materials (top); boundaries of the above-described formulations of zones of failure (bottom)

9. Next, the cohesive crack model (Fictitious crack model [17]) is utilized to introduce the cohesive stresses into the procedure of FPZ extent estimation. In agreement with the cohesive crack approach, the FPZ is supposed to extend from the zone of the current failure around the current crack tip (at stage i, denoted as $\Omega_{\mathrm{PZ},i}$), where the selected stress state characteristics (equivalent stress σ_{eq}) exceeds the tensile strength f_{t}, up to a point on the crack faces where crack opening displacement reaches its critical value (i.e. where the cohesive stress value drops to zero). This point corresponds to a prior stage in the fracture process (which can be denoted by the subscript k, and the zone of failure corresponding to that stage as $\Omega_{\mathrm{PZ},k}$). For a given stage i the FPZ is considered to be a union of zones Ω_{PZ} with subscripts from the interval $\langle i, k\rangle$.
   Two alternative FPZ expressions are considered in the procedure. In the first case, the FPZ is denoted as $\Omega_{\mathrm{FPZ,basic}}$ and the union of the plastic zones from interval $\langle i, k\rangle$ is performed simply without any other treatment. In the other case, $\Omega_{\mathrm{FPZ,scaled}}$, the zones for the individual indices are scaled by a factor corresponding to the relative cohesive stress value for those points, i.e. by $\sigma_{\mathrm{coh}}(w)/f_{\mathrm{t}}$.
   The envelope of Ω_{PZ} zones for a certain stage i of the fracture represents a region in which some sort of damage has taken place during the fracture process up to this stage. That area is referred to as the cumulative damage zone (CDZ) for that stage and is denoted here as $\Omega_{\mathrm{CDZ},i}$. The envelope of plastic zones for all stages of the fracture process throughout the entire specimen ligament is denoted here as Ω_{WRAP}.
   The structure of an FPZ evolving during fracture in quasi-brittle materials is illustrated in Fig. 5 right. The thick solid line in the graph indicates the initial crack face and the front and back boundaries of the specimen. The other lines correspond to the boundaries of the zones described above: the plastic zone $\Omega_{\mathrm{PZ},i}$ for the current crack tip position (point i); the plastic zone $\Omega_{\mathrm{PZ},k}$ for the last crack tip position (point k), where the cohesive stress is still active at the ith step of the fracture process; the fracture process zone Ω_{FPZ} (i.e. the union of plastic zones within the range of action of the cohesive stress) in two considered variants of its representation (basic vs. scaled); and

the envelope Ω_{WRAP} (i.e. the union of plastic zones for all crack tip positions along the specimen ligament – the area where the material undergoes damage). The cumulative damage zone $\Omega_{\mathrm{CDZ},i}$ is not particularly indicated in the figure for its clarity. However, it can be easily recognized according to the description above as the union of $\Omega_{\mathrm{FPZ},i}$(basic) and the tail of Ω_{WRAP} in the figure.

10. The final steps of the procedure deal with the specification of the portions of the work of fracture by appropriate characteristics of the crack and the FPZ. They are under development and testing at present.

A demonstration of some graphical outputs of the procedure is shown in Fig. 6. The evolution of the selected quantities/phenomena corresponding to the stages of the fracture process indicated in the P–d diagram, Fig. 4 bottom left, are displayed in the central area of the SEN-TPB specimen (highlighted in Fig. 4 top left):

- In left column, the Rankine equivalent stress distribution (principal stresses σ_1) within the specimen is depicted. From this picture, one can estimate the extent of the plastic zone, i.e. the zone of material damage that initiates at the current load step. The stress level corresponding to the value of tensile strength, which creates the boundary of the plastic zone, is displayed in the darkest colour.
- Extent of the fracture process zone, i.e. of the area where the cohesive stress is active is shown. Both representations of the zone considered in this work (i.e. basic and scaled) are depicted (middle columns). The intensity of the cohesive stress is indicated by colour scale – cyan indicates that the cohesive stress value is equal to tensile strength; black corresponds to zero cohesive stress.
- The extent of the area where the material undergoes damage, denoted here as CDZ (right column). It is created as an envelope of the plastic zones in stages of the fracture process preceding the current one.

For the construction of the zones, four terms of the Williams power series and the Rankine failure criterion (in plane stress state) are taken into account – such settings have been proven to be applicable in previous studies [53]. Values of coefficients A_1 to A_4 for their evaluation were taken from [24].

It should be noted that further research on several issues of the procedure is planned. For instance, the cohesive function (within the item 9 in the list above) is considered to remain unvarying during the fracture process, which is not in agreement with assumptions stated within the hypothesis. This aspect could be possibly solved by some kind of a model-updating technique. Also, the procedure of the 'plastic' zone determination (within the item 7) does not take into account the stress redistribution. This phenomenon should be incorporated in the procedure as well as the consideration of the non-uniform distribution of the energy dissipation within FPZ.

5 CONCEPT OF VERIFICATION AND VALIDATION OF THE PROPOSED APPROACH

The novel ReFraPro model has been introduced recently by the author and his collaborators. The approach has the ambition to eliminate the drawbacks of the existing models for quasi-brittle fracture description. It shall be achieved via a (detailed) incorporation of the FPZ existence into the method for determination of fracture parameters. These should be then evaluated as the less possible dependent on the specimen size and shape, the notch length, and the boundary conditions of the test.

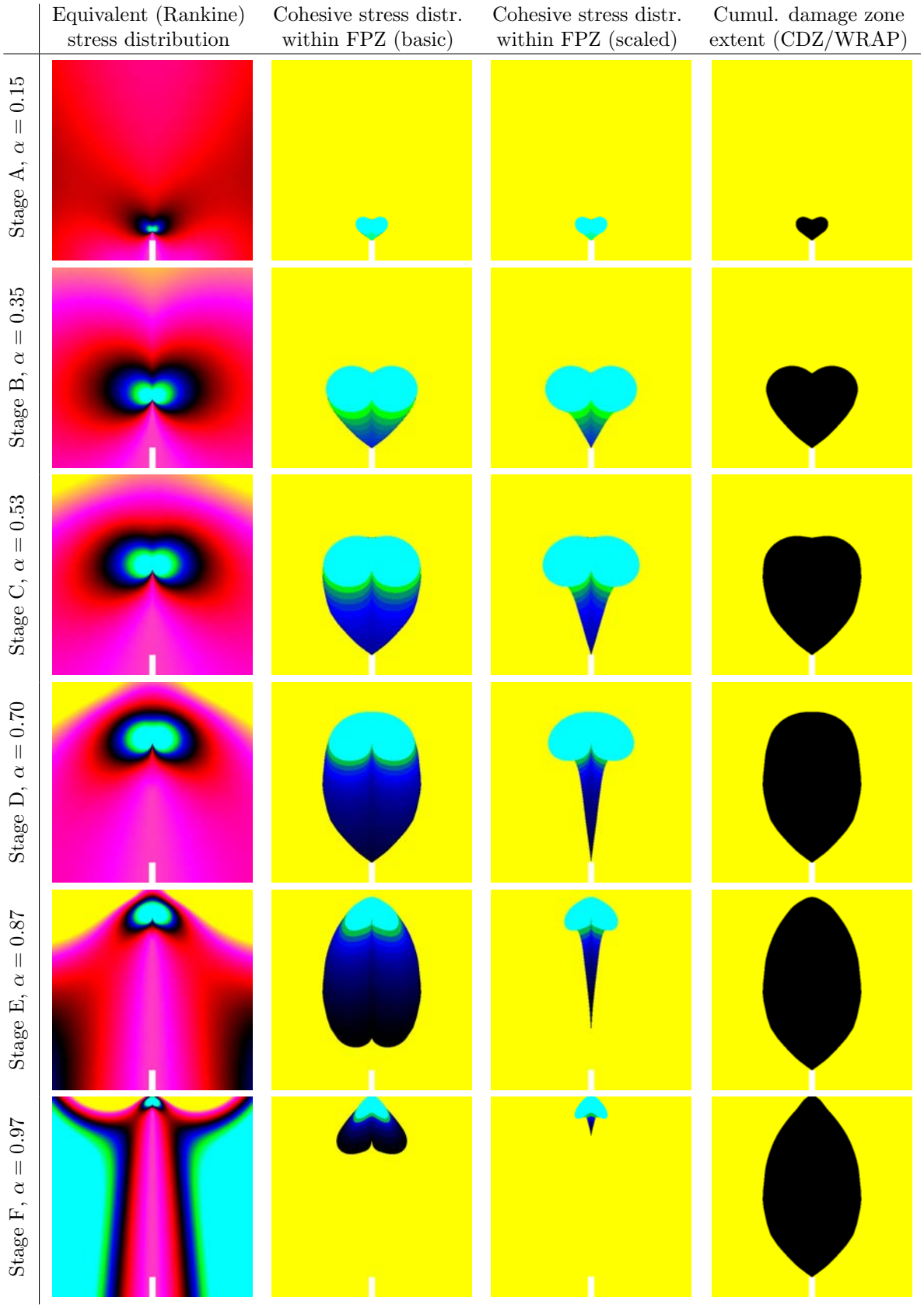

Fig. 6: Central part of the SEN-TPB specimen displaying the evolution of the equivalent (Rankine) stress distribution, the FPZ extent in both the basic and the scaled expression with indications of the intensity of the cohesive stress within it (cyan = f_t, black = 0), and the CDZ extent for the six stages of the fracture process indicated in the P–d diagram in Fig. 4

Results of the method (details given further in the text and particularly in the full version of the thesis) may be regarded as very promising up to now, however, a sound experimental validation still lacks. And this is caused by the fact that most experimental data available in literature are either/both obtained from tests with a limited range of constraint levels (i.e. the FPZ shape/size does not differ as much as it would be necessary to become conspicuous and take it into account for the fracture behaviour evaluation) or/and processed into a form that is not suitable for validation of the method (cumulative extents of the failure zone are mainly published instead of the current ones needed).

To perform a sound validation of the method and its comparison to the existing fracture-mechanics evaluation procedures, an experimental campaign focused on investigation of fracture processes in cases with various extents of FPZ (widths, lengths, of various shapes), and thus various progresses of energy dissipation within it, needs to be conducted.

5.1 Proposal of experimental campaigns

5.1.1 Component wedge splitting/bending fracture test

For one variant of such a campaign, a novel fracture test geometry utilizing combined boundary conditions of the Wedge Splitting (WS) and Tree-Point Bending (TPB)/Four-Point Bending (FPB) test is intended to be used. Detailed description of the test configuration is provided in the full version of the thesis. It is expected that this geometry, via adjusting the specimen length to width and the span to length ratios (and/or simultaneously the wedge angle), will provide a wide range of various stress distributions in the specimen ligament – from bending to a tension with (very) low eccentricity – resulting in the desired variety in the FPZ size and shape. Note that other available test geometries providing a low level of constraint, typically the tension of single or double edge notched specimens (or with central notch), are straightforward for the fracture parameters evaluation, however, very demanding (particularly on the testing machine stiffness and fixtures); therefore, not many relevant results are available in literature (e.g. [1] or [38]).

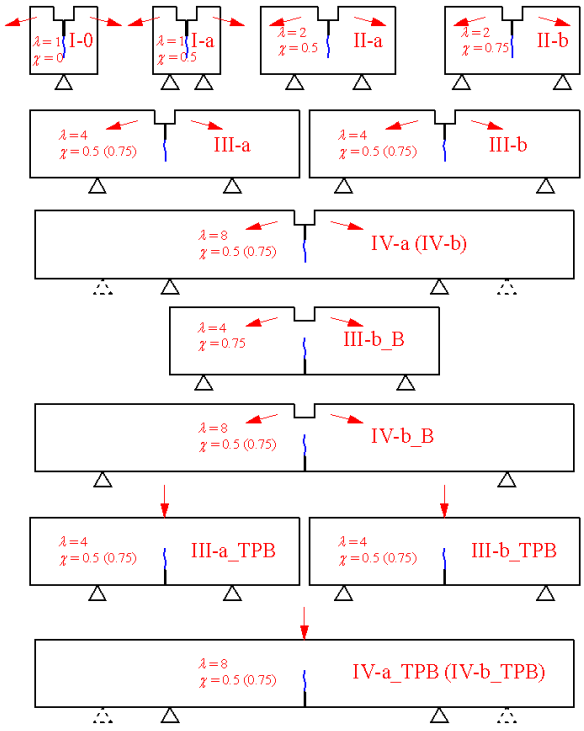

Fig. 7: Set of specimen shapes proposed for the study (from I to IV); variants marked with 'a' are of span to length ratio $\chi = S/L = 0.5$, 'b' of $\chi = 0.75$; if the notch is from the bottom side, 'B' is added; for classical three-point bending 'TPB' is added; the specimen slenderness is characterized by the length to width ratio $\lambda = L/W$; adopted from [49]

Series of geometry variants of mentioned proposed novel test configuration is illustrated in Fig. 7. It is based on the loading mechanism utilized in the wedge splitting test (WST), however, the location of supports and the specimen length varies. Therefore, the combined wedge splitting and bending load is applied. The nomenclature indicated in the figure is introduced for better orientation in the variants of the specimen shapes and boundary conditions.

This experimental campaign is under preparation and pilot testing, proposal for funding has been submitted. Numerical simulations on both the crack tip stress field and the failure

zone extent as a support for the testing plan have been already partially conducted [49, 48].

Fig. 8 shows outputs of the preliminary numerical study conducted using cohesive crack model in ATENA software [8]. Specimens made of normal concrete of moderate strength were subjected to virtual test in this geometry. Profiles of the σ_{xx} normal stress component in the elastic loading regime (however, in several cases some stress redistribution is already visible) and the crack pattern at maximal load are depicted for selected variants of the proposed geometry. The stress profiles change from almost pure bending corresponding to I-0 and II-a to tension with low eccentricity in the case of IV-a or III-b_B. Differences in the failure zone extent are also evident.

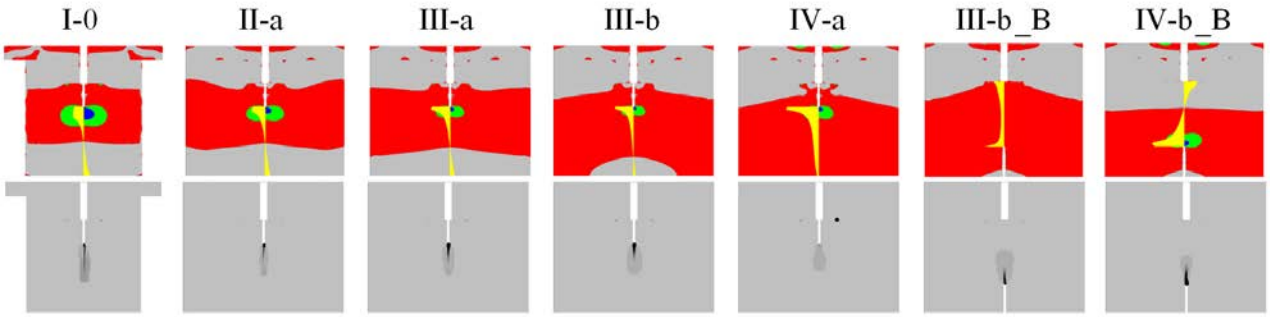

Fig. 8: Comparison of σ_{xx} normal stress isoareas and profiles (at the end of the linear stage of simulated P–d diagram – top) and crack patterns (at peak load – bottom) for the relative notch length $\alpha = 0.3$; middle part of the specimen for variants II to IV is displayed; only tensile stresses are depicted in colours; adopted with changes from [49]

5.1.2 Modification of compact tension test

For other campaign aimed at the same phenomenon, a special modification Compact Tension (CT) test is proposed. The FPZ extent is intended to be observed by X-ray imaging techniques in this case. The measurements will be performed in collaboration with research teams of dr. Daniel Vavřík from the Institute of Theoretical and Applied Mechanics of Academy of Sciences of the Czech Republic, v. v. i. and dr. Jan Jakůbek from the Institute of Experimental and Applied Physics of the Czech Technical University in Prague.

Variations in eccentricity of the tensile forces within the CT configuration cause significant changes in the stress distribution in the tested specimens and hence the level of constraint of stress and deformation near the crack tip, which affects the extent of FPZ [58]. In other words, the level of crack-tip constraint varies with adjustment of the test specimen shape and boundary conditions. How and to which extent this phenomenon can be used for determination of the real values of fracture characteristics of quasi-brittle materials shall be the subject of performed research. Details are covered in the full version of the thesis.

6 VALIDATION VIA AE AND RADIOGRAPHY

Suitable sets of tests were selected for the partial validation of the ReFraPro method from published works dealing with the experimental estimation of the zone of tensile failure in quasi-brittle cementitious composites. Although there are papers focused on the field of FPZ estimation that have been published in recent years, the amount of provided data utilizable without a too excessive effort for validation of the developed ReFraPro procedure is far from massive. Here, attention is paid to experimental techniques based on acoustic emission (AE) scanning under the assumption that AE phenomena are similar to the approach employed

within the proposed method and also due to the fact that AE is the most widely used method in the above-specified field. The results presented hereafter have been published by the author and his collaborators in [51, 52, 46].

In addition, investigation of the material failure employing X-ray imaging is presented in this section. It contains the work published in [50]. Two sets of notched beams prepared from silicate-based composite of two different composition were loaded in three-point bending in a specially designed loading device. Crack length and FPZ shape/size during loading were analyzed using Digital Transmission Radiography (DTR) and X-ray Computed Tomography (XCT). Visualization of the FPZ was enabled using tools of the Digital Image Correlation (DIC) method. These advanced experimental techniques could have been employed due to joint research with groups of the above-mentioned co-workers dr. Daniel Vavřík and dr. Jan Jakůbek.

6.1 Acoustic emission scanning

Mihashi and Nomura [26] tested two sets of WST specimens made of concrete and mortar differing in strength and aggregate size. The experimental set-up with an indication of the specimens' dimensions is depicted in Fig. 9 left. No *P–CMOD* diagrams were reported in the paper and, therefore, own numerical simulations were conducted in order to estimate the structural behaviour of the specimens during the test, which serves as an input for the procedure of FPZ extent estimation. The numerical simulations were performed in ATENA software [8]. The fracture-plastic material model was tuned according to the compressive strength of the concrete reported in the paper.

Two specimens (marked as C10 and C20, maximum aggregate size equal to 10 and 20 mm, respectively) were selected for which the extent of the damage zone was published in the paper. The compressive strength f_c of the concrete of these specimens was equal to 34.8 and 30.5 MPa, respectively. The simulated *P–CMOD* diagrams of specimens C10 and C20 are plotted in Fig. 9 right. Because they are very similar, only one *P–CMOD* curve (the smoothed variant of the C10 one) was used as the input for the ReFraPro procedure. The values of the other necessary input parameters were taken into account as being the same as for the numerical simulation in ATENA: tensile strength $f_t = 2.8$ MPa, fracture energy $G_F = 60$ Jm^{-2}, and Hordijk's exponential softening curve. Four terms of the Williams series and the Rankine failure criterion in a plane stress state were considered.

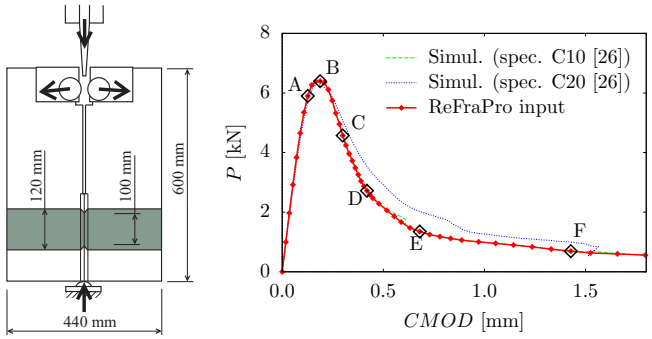

Fig. 9: Experimental set-up and dimensions of WST specimen [26] (left) and corresponding load–displacement diagram (right); adopted from [51, 46]

The second experimental set considered in this thesis was published by Muralidhara et al. in [28]. SEN-TPB tests on two specimens sizes were conducted and accompanied again by AE scanning. From the experiment only one test (the specimen marked as D2T20UB02) was reported in detail in the paper. The test configuration with the dimensions of the selected specimen is shown in Fig. 10 top. From the recorded *P–CMOD* curve present in the paper, the real *P–d* curve was reconstructed using numerical simulation in the ATENA software, see Fig. 10 bottom.

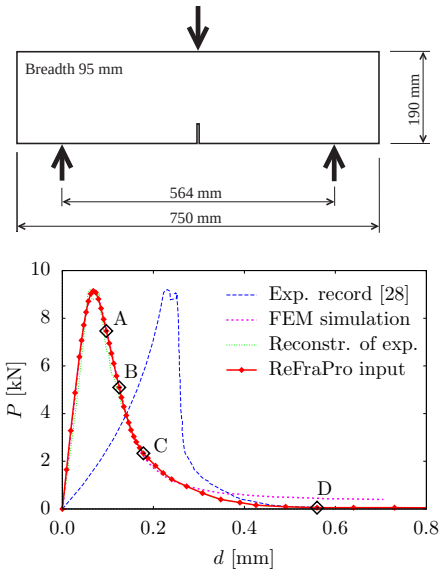

Fig. 10: Test configuration and dimensions of the SEN-TPB specimen [28] (left), load–displacement diagrams (right); adopted from [51, 52]

The parameters of the material model were tuned so that the simulated and experimentally recorded *P–CMOD* curves match. Using the relationship between these curves the 'true' experimental *P–d* curve was subsequently reconstructed, the smoothed version of which was then used as the input for the ReFraPro procedure for the estimation of the damage zone extent. The values of the other necessary inputs to the procedures were again equal to the values of the parameters of the material model used for the simulation: compressive strength $f_c = 42.5$ MPa, tensile strength $f_t = 4.3$ MPa, fracture energy $G_f = 90$ Jm^{-2}, and Hordijk's exponential softening curve. Four terms of Williams' series and the Rankine failure criterion were employed.

6.1.1 Cumulative damage zone extent estimation

The extent of the zones in which the AE sources were located (indicated by the small circles) in the two considered specimens C10 and C20 up to the specific stage of fracture from the experiment [26] is compared to the cumulative damage zone (CDZ) extent predicted by ReFraPro in Fig. 18; for stage B, i.e. the peak load (top), and for the end of the fracture (bottom). Good agreement can be seen, especially for the final stage of the tests.

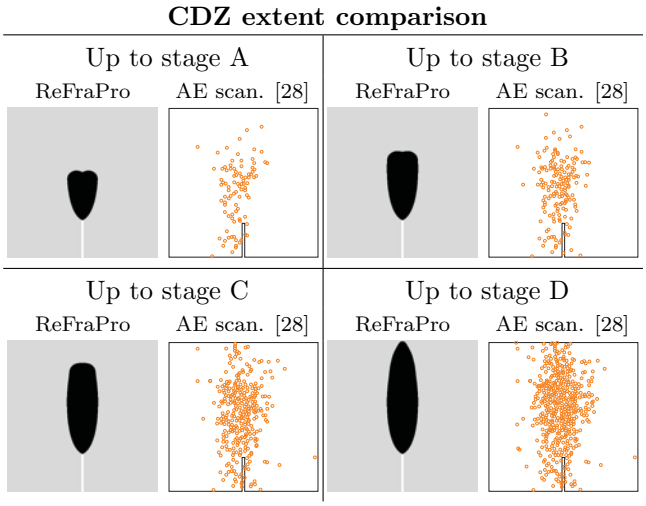

Fig. 11: Central part of the SEN-TPB specimen – comparison of the CDZ extent for four selected stages of the fracture process predicted by ReFraPro with the damage zones estimated experimentally using AE [28]; adopted from [51, 52]

Fig. 11 shows a comparison between the predicted and the measured extent of the damaged zone at four stages of the test from the experiment [28]. The scatter of the AE event locations is higher whilst the density of the AE events is lower (especially for the initial stages of fracture) in the case of the test in [28] in comparison to the tests in [26]. The experimentally estimated extent of the zone of cumulative damage was again predicted quite well.

6.1.2 FPZ extent estimation

The progress of the current FPZ extent with an indication of the intensity of the cohesive stresses within it for six selected stages (emphasized and marked by letters A to F in Fig. 9 right) of the fracture process predicted by the RefraPro method corresponding to the experiment [26] is shown in Fig. 17. No experimental data of this kind, i.e. a current extent of the damage zone corresponding to an arbitrary stage of the fracture process, have been published in [26], the available experimental evidence of the nonlinear zone extent (gained using AE scanning) is presented in the cumulative form only, not in the incremental sense, which would be necessary for proper validation of the FPZ extent modelled by Re-

FraPro[6]. Thus, numerical simulations were conducted towards verification of the current FPZ extent during fracture process. Their detailed description is given in Sec. 7.1.

6.2 Radiographic imaging

6.2.1 Tested materials and specimens, test configuration and equipment

Radiographic investigations of the material failure generally have limits in the dimensions of the test specimens, mainly due to the size of the X-ray detector. In this study, the length of the beam subjected to three point bending was also limited by the chamber diameter of the loading device in which the specimen was placed for the test.

As a material for the specimen preparation, two compositions of a fine-grained cementitious composite was chosen to simulate the failure process of normal-sized building structures/structural members made of concrete, for details see the full version of the thesis. The first specimen set was considered as a pilot testing to develop appropriate methodology of the FPZ and crack analysis intended for future experimental campaign. Specimens were cast into moulds for standard mortar specimens. The specimen selected for the pilot X-ray dynamic defectoscopy (XRDD) analysis presented further in the text was of width W, length L, breadth B equal to 40, 150 and 20 mm, respectively. The loading span S of the test geometry was set to 120 mm, the notch cut using diamond saw was of length $a = 10$ mm.

In the context of the research motivation and targeted conceptual approach introduced in Secs. 2 and 4, specimens of SEN-TPB test configurations of three sizes were cast into moulds designed and manufactured for the second campaign. The design was supported by a detailed numerical study [58]. The study was aimed at searching of an appropriate testing strategy to prove the stated hypothesis, see Sec. 3. The largest size (L) of the beam specimen was the same as in the pilot series, i.e. $W \times B \times L = 40 \times 20 \times 150$ mm, the width W and length L of the middle (M) and small (S) specimen size were scaled by the factor of 1/2 and 1/4, respectively. Breadth B of all specimens remains the same, i.e. 20 mm.

A highly stiff testing device enabling compressive loading developed at ITAM AS CR, v. v. i. was used for the bending tests. This device allows very low loading velocity and its outer dimensions enable X-ray observation of the specimen in the radiographic cabin[7]. Loading device generally consists of the actuating part and of the chamber in which specimen is placed. This chamber was manufactured from two parts. The top section is made from the Certal aluminium alloy and the bottom one from the 0.6 mm thick carbon epoxy laminate, which is practically transparent for X-rays. These parts are connected using bayonet mechanism. Ridges of supports (rollers) of the bending configuration were also prepared from the carbon pins. This solution enables radiographic observation of the analysed specimen without any influence of the loading device for X-ray measurement.

Further details on the testing equipment and procedure of the pilot experiment are described in [50]. The second test series was conducted in CET Telč where the most recent advanced imaging technologies are built in the tomographic system. Unfortunately, strength and stiffness of the material of second specimen set was too hight for the used loading device (the same one as in the pilot experiment) and thus results of the fracture tests were not ob-

[6]Such an analysis is published in [30] where the AE scanning was accompanied also by simultaneous X-ray inspection. However, the sectioning of the whole fracture process into the increments must have been performed much denser. From this point of view, unfortunately, the data can not be used.

[7]The pilot tests were conducted in a radiographic cabin at IEAP CTU Prague, where the dimensions of the loading system played a role. Tests on the second set specimens were conducted at CET Telč, a detachment of ITAM AS CR, v. v. i., where a relatively very large space is available in the X-ray cabin.

tained in a way that could be effectively processed and used for validation of the ReFraPro method. For more details see again the full version of the thesis.

6.2.2 XRDD results

Results obtained in the pilot experiment were very promising. The recorded load–displacement (P–d) diagram is plotted in Fig. 12. Measured force P as a function of both the displacement d_{eng} imposed by the engine and the estimation of the real deflection d of the beam (without displacements taken place at the contacts of the loading chain parts and due to the push-in of supports into the specimen), is showed. The real displacement d was not measured directly, it was determined from X-ray measurements using DIC.

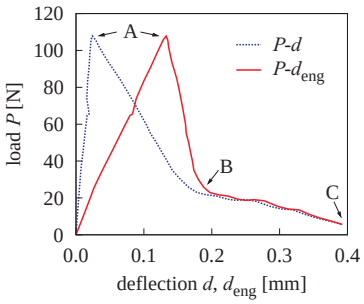

Fig. 12: P–d diagram with indication of stages of FPZ investigation [50]

Radiograms

It is almost impossible to observe FPZ directly in the investigated specimen due to significant internal structure, which corresponds to the natural material inhomogeneity. Therefore, subtractions of the actual and initial radiograms (resulting in the subtraction image) were performed to find changes of the specimen density considering the specimen movement during loading; DIC tools were used for that. Such images are shown in Fig. 13 left (only middle part of the specimen is shown, overturned upside down).

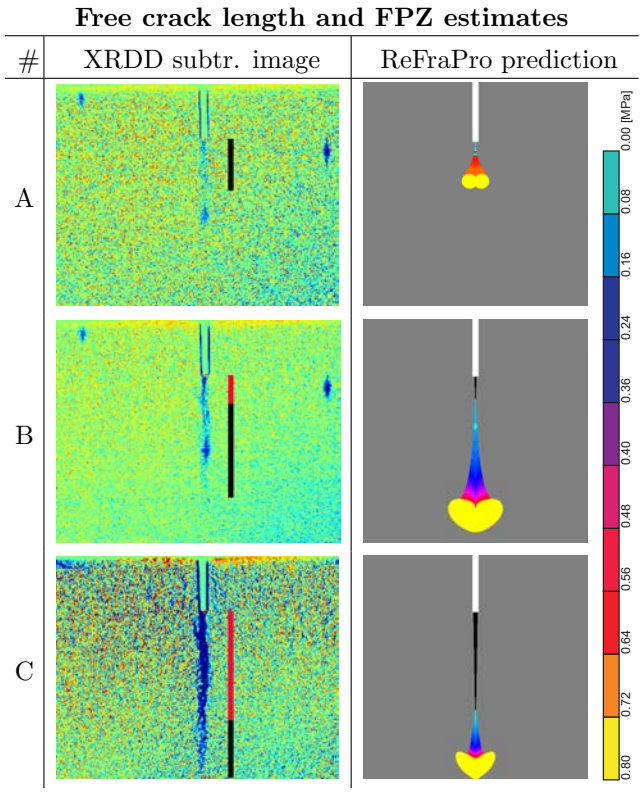

Fig. 13: XRDD subtraction images at the stages A, B and C: The crack and the FPZ lengths are indicated by red and black stripes, respectively (left); corresponding FPZ estimates (with indication of the cohesive stress value) and the free crack using the ReFraPro technique (right); adopted from [50]

It is apparent that the FPZ plays a significant role in the quasi-brittle fracture. In the initial stages of the fracture process, the crack is much shorter than the FPZ. In the case of the A stage, the crack can't be even observed yet and the FPZ length is estimated to 9.3 mm, see top row of Fig. 13. Nevertheless, neither from the subtraction radiogram images the crack and the FPZ can be very easily distinguished. The FPZ extent is represented in the image by a significant change of the specimen density. Although the boundary between the crack tip and the FPZ is, as was already mentioned above, quite blurred, values of the crack and FPZ lengths were estimated to 5.1 and 16.9 mm, respectively, at the stage B. At the stage C, the crack was about 19 mm long and practically whole remaining ligament was weakened by the FPZ. The estimates of the extents of both the stress-free crack and the FPZ for all three investigated loading stages are marked by red and black abscissas, respectively, in Fig. 13.

Results of similar nature were obtained also in the second experimental series. However, due to problems of stability of the

test only indicative results are shown in Fig. 14. It presents radiograms at the start of the test (A), shortly after catastrophic fracture (B) and then in two stages during opening the developed crack (C and D). One of the specimens from the middle sized set is depicted. It is evident that imaging possibilities of the CET Telč workplace are excellent. Repetition of the experimental campaign with more suitable material and upgraded loading equipment is under preparation.

CT reconstruction

The CT measurements in the case of the pilot experiment were done at the emphasized fracture process stages too (the points B and C in the loading curve in Fig. 12). Generally, crack does not follow straight direction and its front is not sharp as it is possible to document using CT reconstruction. It is hard to distinguish which individual voids were born during loading and which were presented from the beginning. However it can be shown, that void density is significantly increasing during loading as presented in Fig. 15 using 3D visualization, stage B left, stage C right. The voids and consequent macroscopic crack are preferentially occurring in the middle of the specimen. Only central part of the specimen containing crack was selected for this visualisation.

Results of tomographic measurements conducted in the unsuccessful second series are not presented here.

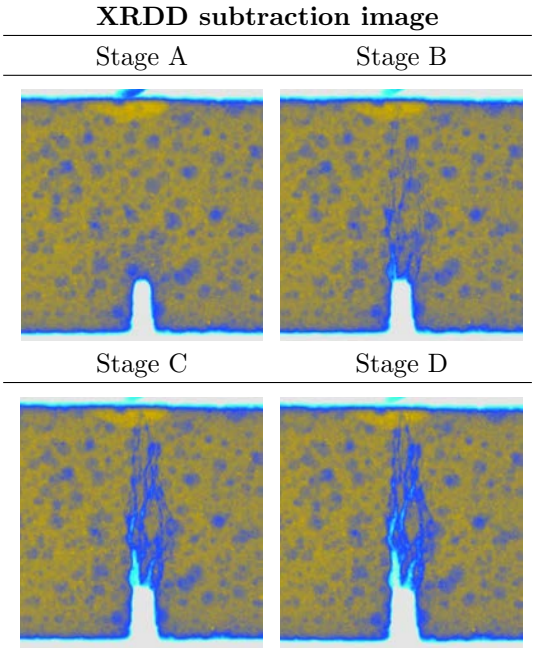

Fig. 14: XRDD images at four stages of fracture process in a selected middle-sized specimen from the second test series

6.2.3 Modelling – FPZ reconstruction

Semi-analytical estimates of the FPZ using ReFraPro method could be validated via the XRDD technique only in the case of the pilot experimental set. The P–d diagram shown in Fig. 12 was used as input into the ReFraPro technique for the estimation of the FPZ extents. Other necessary inputs into the procedure were following: 4 terms of the Williams series, Rankine failure criterion, values of tensile strength f_t (estimated for the tested composite based on inverse analysis using FEM code ATENA) and fracture energy G_f (determined from the recorded P–d curve) equal to 0.8 MPa and 20 Jm^{-2}, respectively, and the exponential (Hordijk's) cohesive function.

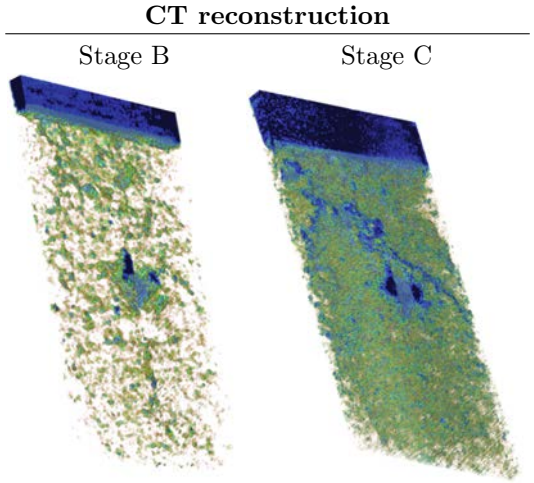

Fig. 15: 3D visualisation of the voids at loading level B (left) and C (right); adopted from [50]

Estimates of the FPZ extent (including the indication of the cohesive stress distribution – from yellow colour corresponding to f_t, to cyan corresponding to zero cohesive stress) and the free crack behind it at the 3 stages of the fracture process (A, B, C) are shown in the right column in Fig. 13 where the comparison to the results of radiographic measurements can be performed.

Nanoindentation presents another technique for the damage zone extent estimation used in this work. Details are covered in the full version of the thesis.

6.3 Discussion on damage zone estimation validation

6.3.1 Acoustic emission technique

Validation of the developed technique is performed only partially here, as most of the experimental data available in the literature usually provide the zones of cumulative failure from beginning of the fracture process to its specific stages, e.g. data published in [39, 40] or [25] (for asphalt concrete). Such zones correspond to envelopes of the FPZs referred to as CDZs within the ReFraPro application. Reasonable agreement in this aspect is observed in the obtained results.

In the case of both investigated experiments, the values of material parameters representing the inputs to the ReFraPro procedure in connection with rather small specimen dimensions resulted in estimation of considerably large FPZ extents and CDZ/WRAP widths. In these cases, a relatively very accurate description of the stress state for the locations far from the crack tip is necessary – it is obtained by using of at least 4 terms of Williams series. For larger specimens and/or more brittle materials less terms may be sufficient. In contrast, for cases where the FPZ takes even larger portion of the specimen's volume it is necessary to describe the stress field even more accurate, i.e. considering more terms of the Williams series.

As has been already pointed out, verification analyses by means of numerical tools of suitable approach, e.g. those based on lattice-particle models, can serve as appropriate complement to the experimental evidence and, therefore, the author's team (mainly dr. Petr Frantík and his collaborators) is involved also in development and utilization of such computational tools. Analyses on verification of the ReFraPro approach by means of this discrete model are presented in Sec. 7.1.

6.3.2 X-ray radiography

The XRDD technique provides an insight into the material structure and can help to observe the decrease of the material density (increase in porosity) in the damaged area at the crack tip. Thus, it can help to answer questions on the length of stress free crack and the volume of the zone weakened by (significant enough) microcracks. On the other hand, this technique is not directly sensitive to stress distribution and resulting energy dissipation. This statements can be illustrated by the comparison of the FPZ interpretations of the XRDD technique and ReFraPro method. It is worth to note in this context that the value of the displayed cohesive stress is inversely proportional to the amount of energy dissipated for the fracture. In the yellow parts of the reconstructed FPZ (the largest ones) the cohesive stress is highest; however, lowest amount of energy is released in the failure mechanisms. And contrary, at the tails of the FPZ (cyan) the maximal energy release is observed.

Reasonable agreement in specific features the FPZ extent and the free crack length given by the model measured experimentally can be reported. In particular, places with the lowest density from XRDD measurements correspond well to places with the highest energy dissipation (i.e. lowest cohesive stresses). The presented type of experimental analysis is planed to be performed on various specimen sizes, test geometries and material compositions in near future.

7 VERIFICATION OF FPZ EXTENT ESTIMATION AND STRESS FIELD APPROXIMATION

7.1 FPZ extent estimation

This section presents analyses on verification of estimation of the size and shape of the zone of material failure evolving around the crack tip during fracture of silicate-based composites. This verification is performed via numerical simulations utilizing several modelling approaches.

7.1.1 Physical discretization method – Rigid body spring networks modelling

Numerical simulations by means of physical discretization of continuum (spring network/lattice-particle type model), and crack band model (a commercial FEM software) are conducted in order to compare obtained outputs with results of the ReFraPro technique, particularly the part modelling the extent of the FPZ. Note that the conducted analyses shall also provide information which are intended to utilize within the other part of the ReFraPro procedure, namely for the specification of the energy dissipated during fracture within the volume of the material undergoing failure (considering its distribution over the volume), which shall provide true fracture parameters of the material.

The discrete spring network model was developed by dr. Petr Frantík from the same institute as the author and has been successfully applied for variety of problems in structural mechanics. It is referred to as FyDiK [13] (from the Czech expression of 'Physical Discretization of Continuum'). The discretization is based on a procedure developed for the Rigid body spring network (RBSN) model, see e.g. [7]. The mass points and the parameters of the translational springs are computed based on Delaunay triangulation and Voronoi tessellation of the specimen volume. Every mass point has its own Voronoi cell, which specifies its mass according to the cell area, material density and thickness. Similarly, the cross-sectional area of the contact edge between two neighbouring Voronoi cells determines the stiffness parameters of the translational spring crossing this edge. The model is then defined as a nonlinear dynamical system described by equations of motion including damping. The solution is conducted explicitly; huge computational demands are handled by parallelization of the code.

7.1.2 Finite element method modelling

The cohesive crack approach modelling is conducted using ATENA nonlinear FEM software [8] based on smeared crack approach. This tool utilizes principles of nonlinear fracture mechanics, damage and plasticity and in both 2D and 3D versions it is widely used in engineering computations. The fracture-plastic constitutive model referred to as *3D non Linear Cementitious 2* was employed in conducted analyses.

7.1.3 Numerical study

Study on numerically simulated fracture responses of WST from [26] were performed. The FyDiK model enabled simulation of the progress of failure in the selected specimen. In order to study the energy dissipation phenomena, 10 realizations of the FyDiK model of the test specimen were created, each of them made of homogeneous elastic isotropic material of specific gravity $\rho = 2400$ kg/m^3, modulus of elasticity $E = 33.0$ GPa, tensile strength $f_\mathrm{t} = 2.0$ MPa, compressive strength $f_\mathrm{c} = 31.45$ MPa and fracture energy $G_\mathrm{F} = 60$ Jm^{-2}.

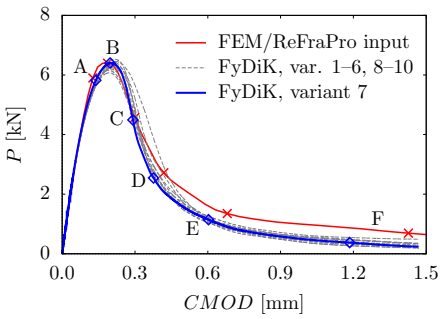

Fig. 16: *P–CMOD* curves from FyDiK simulations; adopted from [46]

Ten variants of discrete model with random mesh (triangular lattice and tessellation structure, respectively) were simulated to take into account the disordered internal structure of the investigated quasi-brittle material, i.e. to 'average' it or to get closer to an isotropic case. During the simulation, both the mutual horizontal displacement of the two points near the mouth of the notch, i.e. *CMOD*, and the splitting force P were recorded, as well as the amount of dissipated energy caused by exceeding the defined value of critical elongation u_{crit} of the individual translational springs. The simulated *P–CMOD* diagrams are shown in the graph in Fig. 16. The loading curve from the FEM simulation by ATENA (serving as an input into the ReFraPro procedure as well) is included there for a comparison.

Relevant details on the testing campaign and performed simulations are given in the full version of the thesis.

The evolution of the FyDiK interpretation of the FPZ in the selected variant of the model (variant 7) is depicted via a sequence of 6 stages of the fracture process in Fig. 17 bottom. These FPZ interpretations are compared to the ReFraPro predictions of the FPZ in corresponding stages of the fracture process (indicated also in the *P–CMOD* diagram in Fig. 9) there. The locations of the individual failure events within each displayed analysis are indicated by spots in the images and coloured according to the amount of dissipated energy.

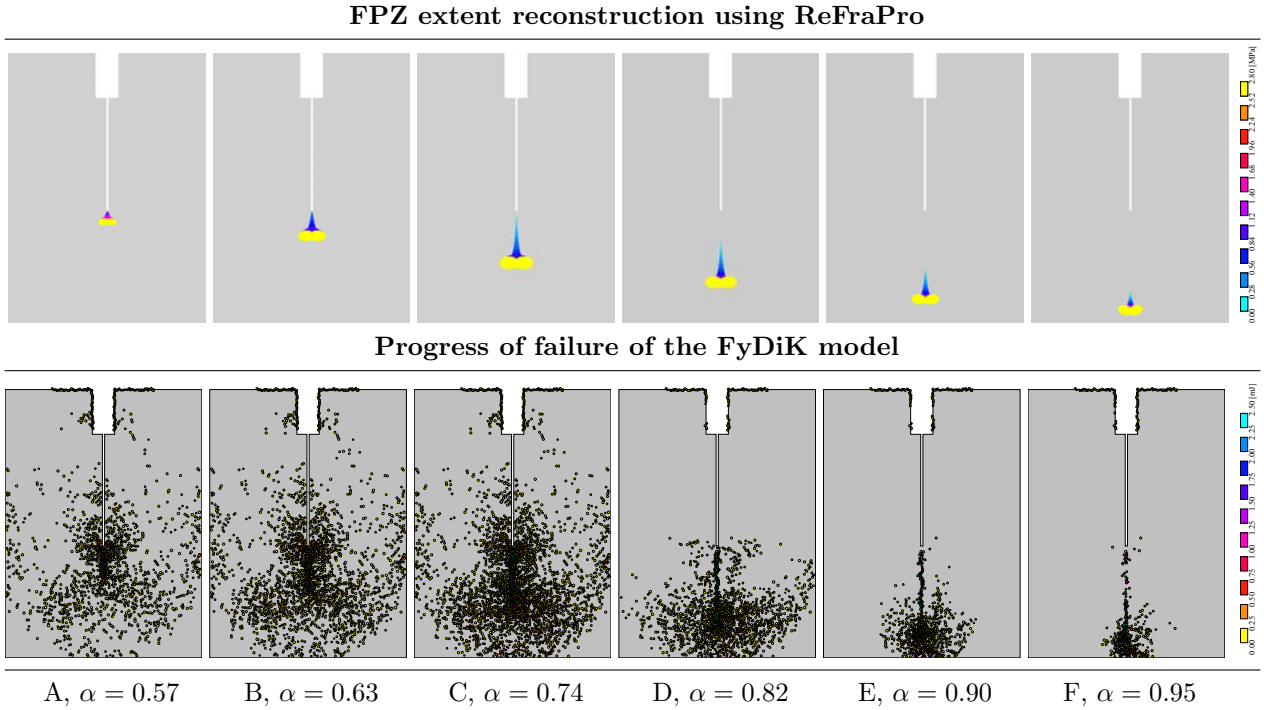

Fig. 17: Top: ReFraPro estimation of the FPZ extent for selected stages of the fracture process (see points A to F in the *P–CMOD* diagram in Fig. 9) corresponding to the selected relative effective crack lengths α with an indication of the modelled cohesive stress intensity; bottom: evolution of the FPZ extent simulated by the FyDiK model for corresponding stages of the fracture process (see points in *P–CMOD* diagram in Fig. 16); adopted from [46]

The size of the spots corresponds with the length of the associated spring (where the energy is dissipated). The term 'dissipated energy' refers to the energy released by the failure of the (softening) particles' bonds creating the model. The FPZ is represented here as a union of failure events which took place within time periods corresponding to localizations of effective crack lengths matching the beginning and the end of the action of the cohesive stress function along the specimen ligament. These effective crack lengths were chosen in agreement with the ReFraPro procedure. In other words, the cumulative number of failure events for the effective crack length corresponding to the critical crack opening w_c of the cohesive function $\sigma(w)$ is subtracted from the cumulative number of failure events for the current effective crack length (where $w = 0$ and $\sigma(w) = f_t$). Thus, a comparison of the FPZ interpretations resulting from this approach and the ReFraPro technique (Fig. 17 top) can be made.

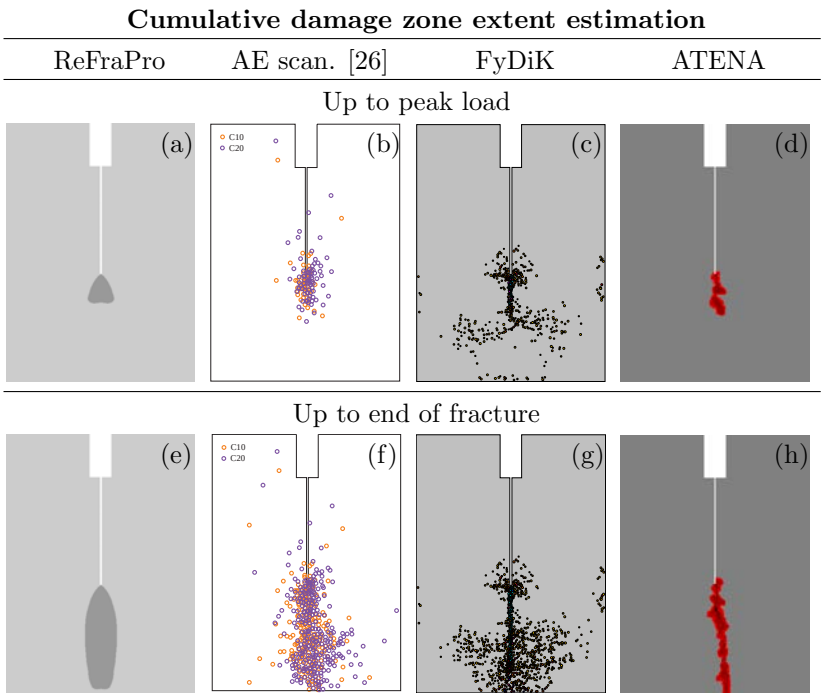

Fig. 18: A comparison of the CDZ extents for two stages of the fracture process estimated (from left): using ReFraPro method – (a) and (e); experimentally using AE scanning [26] – (b) and (f); by means of FyDiK model simulation – (c) and (g); using ATENA FEM model – (d) and (h); adopted from [46]

A comparison of the considered approaches for the estimation of the cumulative damage zone extent can be performed as well. In Fig. 18, the CDZs are compared for both the stage of the fracture process corresponding to the peak load (top row) and its end (bottom row).

7.2 Approximation of stress field in cracked bodies

This part is aimed at the approximation of the stress and displacement fields both in the vicinity and also at a larger distance from the crack tip in test specimens utilized for the determination of the fracture characteristics of quasi-brittle materials. Studies on quality of the multi-parameter approximation of the stress fields around a crack tip in a non-brittle material test specimens are introduced in the full version of the thesis, here only selected examples are shown. The stress field approximation using Williams power series is intended to be utilized for estimation of the nonlinear zone extent which potentially plays a role within methods for determination of true values of fracture parameters of materials exhibiting nonlinear failure. Considering the fact that in the case of elastic-plastic and especially quasi-brittle materials the size of this zone is substantial in comparison to the specimen dimensions, it is necessary to take a large region around the crack tip into account for this task.

Determination of values of coefficients of the higher order terms of Williams power series was performed via the over-deterministic method (ODM) [4] applied on results of finite element analysis of selected mode I test geometries. The ODM was implemented in MATHCAD

mathematical package and later, in order to facilitate further conducted analyses, also in JAVA programming language as a multi-platform and object-oriented computational tool.

Another Java application employed within the studies present in this section is a tool for plotting the stress distribution over the specimen in the form of isolines and contour plots. It is a subroutine of the ReFraPro package and provides a backward reconstruction of the crack-tip stress field analytically by means of truncated Williams expansion.

Several case studies involving various aspects of the solved problem of crack-tip fields description have been carried out. Here, selected results are introduced. The agreement between the analytical and numerical solution with regard to the distance from the crack tip and the number of terms of the Williams expansion that were taken into account in the analytical expression is discussed.

7.2.1 Numerical study

A novel test geometry has been proposed by the author and his collaborators in [54]. In fact, the hybrid test configuration is derived from two basic and most frequently used test configurations utilized for the determination of fracture properties of quasi-brittle materials: the bending of notched beams and the wedge-splitting of (usually) compact specimens. Diagram of variants the proposed configuration is depicted in Fig. 7.

The WST geometry forms one boundary of the considered study. The other asymptote is the three-point bending (when the specimen size becomes large enough to neglect the width of the WST fittings and the groove for their insertion). However, for relevant laboratory specimen sizes it is necessary to deal with a combination of the wedge splitting (tension in the top parts of the specimen ligament and compression in the bottom ones) and four-point bending (vice versa) tests. As such, the stress state in the specimen ligament can be controlled by adjusting the test configuration parameters (e.g. loading span S, specimen width W, and the wedge angle α_{w}). A broad range of crack-tip constraint level, and consequently also extents/shapes of the nonlinear zone evolving around the crack tip, can be obtained.

FEM model

The elastic stress and displacement analyses in the studies were conducted in the ANSYS FEM software [3] by Ing. Jakub Sobek. All simulations were modelled in 2D under plane strain conditions. The FE mesh was generated from 8-nodes isoparametric elements (PLANE82), with the crack-tip singularity taken into account via triangular crack elements with the mid-side node moved to 1/4 of the length of side of triangular element. Linear elastic isotropic material of the cementitious composite specimen and the steel loading platens was defined by Young's moduli $E = 35$ and 210 GPa and Poisson's ratios $\nu = 0.2$ and 0.3, respectively.

Stress field reconstruction

In order to investigate the influence of the higher-order terms on the stress distribution in specimen variants of the proposed test configuration, the stress tensor components have been plotted over the specimen area and compared to FEM result, which is for this analysis regarded as the exact solution. Note that the FE solution results served as inputs to the ODM from which the values of the higher order terms were calculated.

Selected results of the study for the the classical WST specimen are shown in Fig. 19. For the relative crack length value $\alpha = 0.2$ and $\alpha = 0.5$, and the stress tensor components σ_{yy} and σ_{xx}, respectively, the fields are analytically reconstructed via Williams power expansion truncated to various ranges of its initial terms, namely $N = 1$, 2, 4, 7, and 12, respectively.

These fields reconstructions are interpreted through isolines and can be compared to FE solution expressed as contour plots. In some cases, mostly for the higher values of the last considered term N, certain regions (sectors of certain range of angle θ) are observed where no solution of the plasticity condition was found within a distance from the crack tip r smaller than that of the specimen boundary. In these cases the stress isolines, particularly for larger distances from the crack tip, are not continuous. This effect is extremely visible in the case of high value of N and low value of the investigated stress tensor component.

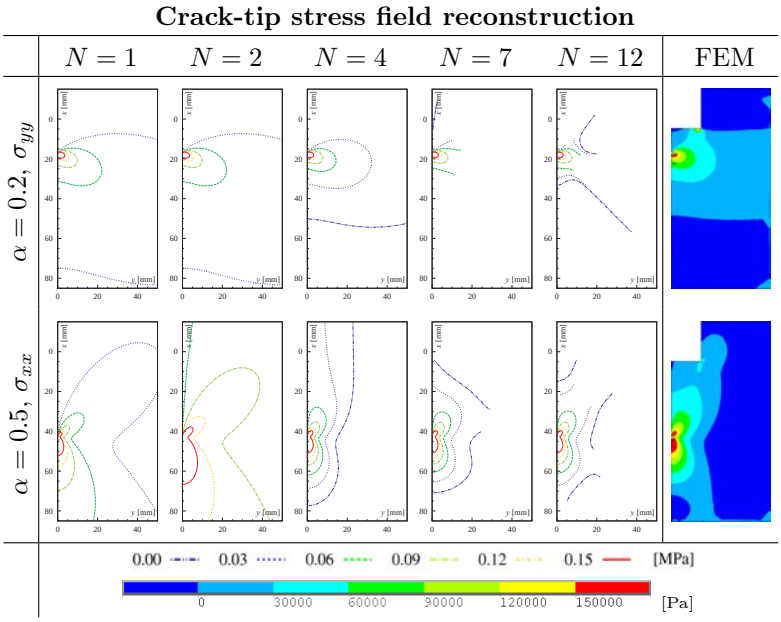

Fig. 19: Comparison of stress fields (from top σ_{yy}, σ_{xx}) reconstructed by means of Williams series using various ranges of terms (from left 1, 2, 4, 7, and 12, respectively) with the FEM solution; adopted from [59]

Nonlinear zone width estimation

A simplified representation of the nonlinear zone width is studied in this section. This simplification is mainly due to the fact that no stress redistribution is taken into account and the 'plastic zone' is constructed in analogy with technique used in fracture mechanics of metals when small-scale yielding condition applies.

Comparison of the analytical reconstruction and the FEM solution of the stress field for a selected test geometry is performed, classical WST is investigated. In these cases, filled-plane contour plots are shown. The iso-stress contours may represent a nonlinear (plastic) zone extent provided when the Rankine failure criterion was applied.

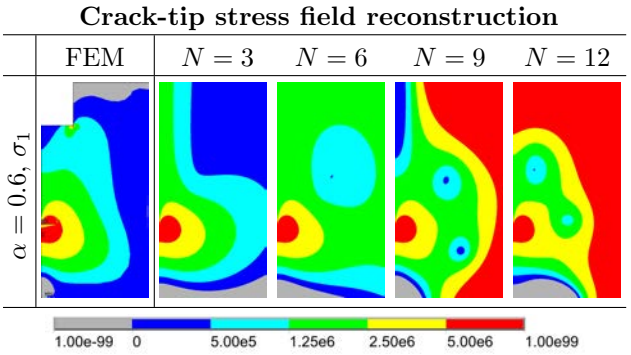

Fig. 20: Comparison of σ_1 stress field for the selected relative crack length $\alpha = 0.6$ reconstructed by means of Williams power expansion using several ranges of terms of the series with the FEM solution; adopted from [54]

7.3 Discussion on FPZ estimation and stress field approximation

7.3.1 Verification of FPZ estimation

Materials with monotonic softening

The overall extent of the failure zone estimated using the ReFraPro technique fits the experimental data well, especially for the end of the fracture. Likewise, the FPZ extents by ReFraPro and results of the FyDiK simulation of the current damage zone extent are also in reasonably good agreement.

The area of the damaged material resulting from the ATENA simulation is considerably narrower than that estimated experimentally and by the ReFraPro method. Nevertheless, it corresponds well with the area where failure events with a high amount of energy dissipation take place in the FyDiK simulations.

The region of the acoustic-emission-like events' locations provided by the FyDiK fracture model captures the experimental data well; the distribution function of the intensity of the energy dissipation, however, needs to be validated experimentally (e.g. by approach similar to [16]).

From the comparison of the evolution of current FPZ extent by means of the ReFraPro technique and the FyDiK model it is obvious that the size and shape of the FPZ reconstructed by the ReFraPro technique is realistic. The character of the FPZ shape was captured quite well, though its size seems to be overestimated. Nevertheless, it should be noted that the conclusion is achieved via the from comparison of different quantities and should be regarded as provisional. Subsequent analyses of the results are planned. This research shall include studies regarding the cohesive stress distribution over the FPZ, with which the energy dissipation is connected. Moreover, a stress redistribution at the crack tip has not been considered within the ReFraPro technique yet.

Strain hardening materials

An analysis similar to that presented in this shortened version of the thesis have been conducted also with strain hardening cementitious composites. In these cases, quite reasonable agreement between the FPZ estimations obtained by the two approaches was observed only for the bilinear cohesive function (of a reference material). The agreement is both in the characteristics of the FPZ extent (the size and shape) and the parameter describing the failure intensity (the intensity of cohesive forces and energy dissipation, respectively). Generally, better agreement was obtained for larger specimens (due to denser mesh of the FyDiK model).

The confrontation of results of simulations with trilinear cohesive functions (strain hardening materials) was not satisfactory, especially regarding the tail of the FPZ; the estimation of the front part of the FPZ is in most cases more successful. The observed discrepancy is most likely connected with the (up-to now) not satisfactorily resolved issue of incorporation of the cohesive function in the procedure of FPZ estimation within ReFraPro.

Besides, the straightforward comparison of the intensity of energy dissipation (FyDiK representation) and the cohesive stress distribution (ReFraPro representation) is not completely appropriate; update of the analysis is planned in future research.

In some cases, mainly for small specimens, a non-smooth boundary of the FPZ extent was observed. It is caused by the insufficiently accurate description of the stress state; additional terms of the Williams series should have been taken into account in the ReFraPro procedure in these cases.

7.3.2 Verification of stress field approximation

Reconstruction of stress field

From the comparison of the plotted stress field approximations using truncated Williams power series with the FEM solution, it is clearly visible that the description of the stress field farther from the crack tip provided by low number of terms of the series is very inaccurate. On the other hand, increasing number of the terms leads to worse stability of the power series approximation, the stress function fluctuates very much in certain sections of the investigated space (considering the polar coordinate system). In particular, following points are worth emphasizing:

- Description of the stress fields using only the first or the first two terms of Williams power expansion is feasible only in very small region around the crack tip.
- With increasing the distance from the crack tip also the number of terms necessary for keeping reasonable accuracy of the description increases.
- At larger distances from the crack tip, the stress field reconstruction provided by high number of terms of Williams power series may start behave in rather uneven manner, which complicates its utilization within fracture analysis.
- Suitable number of terms of the Williams series which should enter the fracture analysis depends on mutual relations of the specimen size and shape, applied load, strength limit and the investigated component of the stress tensor. In other words, on the proportion of the size/shape of the region where the failure takes place to the specimen boundary. The type of failure condition influences the choice as well. But generally for the conducted studies, the number of terms N should be greater than or equal to 4.

Discussion of the results of the stress field reconstruction is based only on the visual comparison of the contour plots in this work. It is intended to apply a suitable method for the inaccuracy quantification in further research.

Estimation of nonlinear zone width

The nonlinear (plastic) zone extent could be estimated using several relevant yield criteria. For analyses presented in this work, the failure criteria considering internal friction in the materials are typically used as cement-based composites are the primary materials in question. Thus, the Rankine failure criterion ($\sigma_1 \leq f_t$) or even simply the crack opening stress criterion ($\sigma_{yy} \leq f_t$) can be taken into account here.

Fig. 20 can be named as an example for that analysis. If the strength limit of the material were about 2.5 MPa, around 6 to 9 terms would be necessary for a sufficiently accurate description of the nonlinear zone. It can be seen that the solution suffers poor stability similarly to analyses discussed in previous section. It is again observed that with increasing N, the results of the analytical reconstruction of the stress fields are refined close to the crack tip and become disrupted farther away from it.

8 CONCLUSIONS AND OUTLOOKS

8.1 Conclusions – FPZ and WRAP extent validation

8.1.1 Acoustic emission technique

Experimental techniques utilizing AE have a great potential to answer the key questions related to the initiation and propagation of failure in quasi-brittle materials, which is connected with the evolution of FPZ at the tip of the propagating macroscopic crack. The ReFraPro method has been partially validated using experimental data from the literature which were obtained by the AE technique. However, the limited amount of experimental evidence together with the deficient range of the published data and the way of their processing resulted in a need for numerical simulation of the AE phenomena triggered by the tensile failure in the material. Particularly, the cumulative expression of the damage zone, not the current one which is desired for the ReFraPro estimation of the FPZ extent, is typically published (a rare exception can be found in [16]). Therefore, the FyDiK discrete model was used to accompany analyses on the FPZ extent estimation.

8.1.2 Radiography

It was proven that X-ray radiography in combination with DIC and CT reconstruction are powerful tools for analysing of the crack and FPZ evolution during fracture of quasi-brittle specimen. Experimental results showed that FPZ is significant in comparison with the macroscopic crack length in the case of the tested material and specimen size. Agreement between the results of ReFraPro procedure for the FPZ extent estimation and the experimental observations was obtained in some aspects, however, further research is needed (regarding e.g. the interpretation of the energy dissipation etc.).

8.1.3 Nanoindentation

The extent of the material damage due to external loading was attempted to be identified by changes in mechanical parameters determined by nanoindentation technique, particularly by the decrease in Young's modulus. The surface fluctuation of this mechanical parameter was evaluated, and from it the boundary of the damaged material zone was assessed. The conducted nanoindentation experiments showed feasibility of the method based on the measurement of the decrease in local micromechanical properties across the crack; however, for the tested cementitious composites with considerable heterogeneity of the material resulting in disordered manner of fracturing, the width of the nonlinear zone has not been reliably determined.

8.2 Conclusions – Crack-tip stress field and FPZ extent verification

8.2.1 Crack-tip stress field approximation and nonlinear zone width estimation

It has been found out that higher-order terms of the Williams power expansion derived for the description of the stress/displacement field in a cracked specimen play a key role if a knowledge of accurate stress/displacement fields not only very close to the crack tip is required. Sufficient number of higher-order terms necessary for accurate stress and displacement field description within a body with a crack depends on the size of the region in question; the studies show that definitely more than one or two terms, which are used conventionally within the well-known one- or two-parameter fracture mechanics, should be taken into account.

Component wedge splitting/bending test geometry
Analysis of the stress and displacement fields near a crack tip in a component wedge splitting/bending test geometry specimens was presented. The influence of the specimen shape and boundary conditions on the coefficients of higher-order terms of the Williams series (up to the order of 12) was investigated.

Various ranges of the terms were subsequently used for the analytical reconstruction of the stress field around the crack tip and were compared with stress distribution obtained by means of the FEM. The results clearly show that especially for short and long cracks and/or at larger distances from the crack tip the accurate approximation of the stress field requires the use of more terms of the Williams expansion. Unfortunately, increasing number of the Williams expansion terms leads to worse stability of the power series approximation and, therefore, the accurate stress field description in some directions from the crack tip is not always easy to obtain.

Computed results indicate that the studied specimen shapes and the location of the load application at the upper surface or/and supports at their bottom surface affect the values of the shape functions $g_{\mathrm{n}}(\alpha)$ (functions of the coefficients of the higher order terms of the

Williams series) to a rather significant extent. Changes in specimen proportions or/and the positions of loads/supports influence slightly the crack-tip constraint level resulting in possible differences in the width of the nonlinear zone. The stress field becomes less constrained with increase in the length of the specimen and the span between supports. However, in such cases the nonlinear zone width increases only slightly.

Accuracy of crack-tip fields approximation in WST

In this study, general issues regarding the stress field approximation around the crack tip in a 2D body loaded in mode I were discussed; a variant of WST specimen was taken as an example.

The way of selection of the nodal results from the FEM solution as the inputs to the ODM on the quality of the final stress field capturing and its backward reconstruction was investigated. Several variants of selecting of the nodes were compared and discussed with regard to the accuracy of the stress field approximation. Significant advantages of the usage of multi-parameter description in the analysis of the stress field were reported; large errors of the approximation caused by a limited number of terms were demonstrated.

Results of this study have significant implications to intentions on estimations of the FPZ extents in quasi-brittle materials. The technique of the FPZ estimation implements the crucial parts of the above-mentioned procedure; functioning of the technique has been/is currently being verified via numerical simulations of the fracture process in the test specimens by means of a lattice-particle (spring network) model and was/is planned to be validated with the help of AE and/or XRDD techniques in future research.

8.2.2 Numerical verification of FPZ extent

Analyses aimed at the verification of the ReFraPro technique for estimation of the extent (size and shape) of the FPZ and the cumulative damage zone in quasi-brittle silicate-based composites during tensile failure were presented. The FyDiK software was successfully employed for that (partial) verification. The modelling approach was applied on materials exhibiting, except from only softening, also rather ductile, even strain hardening, cohesive behaviour.

The ReFraPro method has already been partially validated using AE experimental data from the literature. This validation is just partial due to certain limitations of the published AE data described above from which the need for proper simulation of this phenomenon has arisen. Thus, the FyDiK model was used for estimation of a volume where AE events have been localized, including their energy consumption. The FPZ extents predicted using the ReFraPro and FyDiK approach are in reasonable agreement, both in the characteristics of the size and shape and the parameter describing the failure (the intensity of cohesive forces and energy dissipation, respectively); however, only for softening cohesive functions. In the cases of non-monotonic cohesive functions, i.e. the cases of quasi-ductile or even strain-hardening materials, the agreement was not satisfactory. The width of the damage zone was significantly overestimated.

Both the FyDiK model and the ReFraPro method show promising features utilizable in relevant research areas. The former one provides a fairly good approximation of FPZ and WRAP volume and can serve as a significant source of new knowledge regarding the energy dissipation mechanisms in the FPZ in the case of quasi-brittle materials. The latter one can provide a way how to incorporate the effect of the laboratory test specimen size and shape (and/or its free boundaries) into methods for determination of fracture parameters.

Nevertheless, it should be noted that the conclusions coming out from the presented comparisons should be regarded as provisional; they are achieved via confrontation of different

quantities (the value of cohesive stress in ReFraPro vs. the value of dissipated energy in FyDiK). Subsequent analyses of the results are planned. This research shall include studies regarding the cohesive stress distribution over the volume of the FPZ, with which the energy dissipation is connected.

8.3 Outlooks

8.3.1 Analytical estimation of FPZ extent and the related energy dissipation

A potential fundamental drawback of the proposed ReFraPro methodology, which the author with collaborators are aware of, is the direct combination of the LEFM description of the crack-tip stress field, however, provided in more accurate way than in classical approaches, with the cohesive crack model. Thus, the elastic and nonlinear fracture approaches are mixed. For example, both these theories work with different crack face shapes/lengths (and resulting stress states around the crack tip). The LEFM crack is sharp characterized by stress singularity. On the contrary, the CCM crack, faces of which adhere due to cohesive forces, is generally longer for the same loading situation and closes smoothly with vanishing stress intensity factor. However, fields farther from the crack tip are under consideration in the presented technique as the extent of FPZ is substantially large and it is believed/presumed here that their description via multi-parameter LEFM at and out of the FPZ boundary is correct. This assumption may eventually be proven as too strong and the method would have to be revised; analyses on that issue are planned, nevertheless, based on current results, this problem doesn't seem to be of a great importance.

A possible way how to keep the technique 'pure' is e.g. adopting the formulation from [21, 22] decomposing the cohesive crack-tip stress field into a traction-free (sharp) crack characterized by several initial terms of Williams series and a fictitious crack increment with smoothly closing faces (within this approach it is assumed to be the FPZ length) loaded by 'remaining' cohesive forces resulting from subtraction of the original cohesive forces and the crack-opening stress for the sharp crack. To keep the developed procedure as simple as possible for feasible evaluation of relevant quasi-brittle fracture properties, the simplification on direct combination of LEFM and CCM was adopted. One of the features of the developed ReFraPro procedure that compensates this simplification is that the front of the FPZ (i.e. region where tensile strength of the material is reached) extends further ahead of the (sharp) effective crack tip (see Fig. 5), which makes the situation closer to the CCM response. Note that combination of the equivalent elastic and cohesive crack approaches, similar to that presented in this work, is employed within the double-K model [31, 44, 45], which seems to be frequently utilized at present, judging by a RILEM committee established on this topic in 2011.

Next issue to be fixed is the stress redistribution due to large FPZ in quasi-brittle materials. Techniques enabling remedy for that problem are investigated and discussed e.g. in [35], which may serve as inspiration.

Effort will be also devoted to thorough analysis of modelling/capturing the energy dissipation over the FPZ volume. This issue has been raised in the 'Hypothesis' section (Sec. 3) only and is not adequately covered in subsequent parts. However, it represents an important topic of the author's research at present. Partial results have been already submitted for publication [47], but it can not be yet regarded as a strong enough verification of the approach. The author must admit that, from this point of view, the second part of the story remains untold in the present thesis.

8.3.2 Experimental characterization of FPZ

Deeper analysis of experimental results, both from own measurements and the published data, is intended. Within the AE data processing, it concerns the assignment of the individual fracture events to the individual steps of the test. This should reveal the current extent of the FPZ. The energy dissipation distribution in the FPZ is another important topic. Both these objectives can be investigated via measurement of energetic demands of the individually located AE events.

The author also plans to compare the outputs of the ReFraPro procedure to data obtained by other types of experimental techniques. It's worth noticing here that the author is involved in research into the current FPZ extent observation via X-ray imaging techniques. At present, the results of pilot experiments are available and were presented in Sec. 6; however, a thorough experimental campaign is under preparation, see Sec. 5.

REFERENCES

References to sources from literature

[1] Akita, H., Koide, H., Tomon, M., Sohn, D. (2003) A practical method for uniaxial tension test of concrete. *Materials & Structures*, 36, 365–371.

[2] Anderson, T.L. (2005) *Fracture mechanics: Fundamentals and applications* (Third Edition). CRC Press, Boca Raton.

[3] ANSYS Program Documentation (2007). Version 11.0. Swanson Analysis System, Inc., Houston, USA.

[4] Ayatollahi, M.R., Nejati, M. (2011) An over-deterministic method for calculation of coefficients of crack tip asymptotic field from finite element analysis. *Fatigue & Fracture of Engineering Materials & Structures*, 34, 159–176.

[5] Bažant, Z.P. (1996) Analysis of work-of-fracture method for measuring fracture energy of concrete. *Journal of Engineering Mechanics (ASCE)*, 122(2), 138–144.

[6] Bažant, Z.P., Planas, J. (1998) *Fracture and size effect in concrete and other quasibrittle materials*. CRC Press, Boca Raton.

[7] Bolander, J.E., Yoshitake, K., Thomure, J. (1999) Stress analysis using elastically homogeneous rigid-body-spring networks. *J. Struct. Mech. Earthquake Eng. (JSCE)*, 633, 125–132.

[8] Červenka, V. et al. (2011) ATENA Program Documentation, Theory and User Manual. Cervenka Consulting, Prague.

[9] Duan, K., Hu, X.-Z., Wittmann, F.H. (2003a) Boundary effect on concrete fracture and non-constant fracture energy distribution. *Engineering Fracture Mechanics*, 70, 2257–2268.

[10] Duan, K., Hu, X.-Z., Wittmann, F.H. (2003b) Thickness effect on fracture energy of cementitious materials. *Cement & Concrete Research*, 33, 499–507.

[11] Duan, K., Hu, X.-Z., Wittmann, F.H. (2007) Size effect on specific fracture energy of concrete. *Engineering Fracture Mechanics*, 74, 87–96.

[12] Eliáš, J., Vořechovský, M., Skoček, J., Bažant, Z.P. (2015) Stochastic discrete meso-scale simulations of concrete fracture: Comparison to experimental data. *Engineering Fracture Mechanics*, 135, 1–16.

[13] Frantík, P. (2007) FyDiK application, http://www.kitnarf.cz/fydik, 2007–2015.

[14] Grassl, P., Grégoire, D., Rojas-Solano, L., Pijaudier-Cabot, G. (2012) Meso-scale modelling of the size effect on the fracture process zone of concrete. *International Journal of Solids and Structures*, 49, 1818–1827.

[15] Grégoire, D., Rojas-Solano, L., Pijaudier-Cabot, G. (2013) Failure and size effect for notched and unnotched concrete beams. *International Journal for Numerical and Analytical Methods in Geomechanics* 37, 1434–1452.

[16] Grégoire, D., Verdon, L., Lefort, V., Grassl, P., Saliba, J., Regoin, J.-P., Loukili, A., Pijaudier-Cabot, G. (2015) Mesoscale analysis of failure in quasi-brittle materials: comparison between lattice model and acoustic emission data. *International Journal for Numerical and Analytical Methods in Geomechanics*, 26 p. doi:10.1002/nag.2363.

[17] Hillerborg, A., Modéer, M., Petersson, P-E. (1976) Analysis of crack formation and crack growth in concrete by means of fracture mechanics and finite elements. *Cement & Concrete Research*, 6, 773–782.

[18] Hoover, Ch.G., Bažant, Z.P., Vorel, J., Wendner, R., Hubler, M.H. (2013) Comprehensive concrete fracture tests: Description and results. *Engineering Fracture Mechanics*, 114, 92–103.

[19] Hu, X.-Z., Duan, K. (2004) Influence of fracture process zone height on fracture energy of concrete. *Cement & Concrete Research*, 34, 1321–1330.

[20] Java™. Programming language. http://www.java.com/en/about/.

[21] Karihaloo, B.L. (1995) *Fracture mechanics and structural concrete*. Longman Scientific & Technical, New York.

[22] Karihaloo, B.L. (1999) Size effect in shallow and deep notched quasi-brittle structures. *International Journal of Fracture*, 95, 379–390.

[23] Karihaloo, B.L., Abdalla, H.M., Imjai, T. (2003) A simple method for determining the true specific fracture energy of concrete. *Magazine of Concrete Research*, 55, 471–481.

[24] Knésl, Z., Bednář, K. (1998) *Two-parameter fracture mechanics: Calculation of parameters and their values* (in Czech). Institute of Physics of Materials, Academy of Sciences of the Czech Republic, v. v. i., Brno.

[25] Li, X., Marasteanu, M. (2010) The fracture process zone in asphalt mixture at low temperature. *Engineering Fracture Mechanics*, 77(7), 1175–1190.

[26] Mihashi, H., Nomura, N. (1996) Correlation between characteristics of fracture process zone and tension-softening properties of concrete. *Nuclear Engineering & Design*, 165, 359–376.

[27] Murakami, Y. (1987) Stress intensity factors handbook. Pergamon Press, Oxford.

[28] Muralidhara, S., Raghu Prasad, B.K., Eskandari, H., Karihaloo, B.L. (2010) Quantification of fracture process zone size and true fracture energy using acoustic emission. *Construction & Building Materials*, 24, 479–486.

[29] Nallathambi, P., Karihaloo, B.L. (1986) Determination of specimen-size independent fracture toughness of plain concrete. *Magazine of Concrete Research*, 38, 67–76.

[30] Otsuka, K., Date, H. (2000) Fracture process zone in concrete tension specimen. *Engineering Fracture Mechanics*, 65, 111–131.

[31] Reinhardt, H.W., Xu, S. (1999) Crack extension resistance based on the cohesive force in concrete. *Engineering Fracture Mechanics*, 64, 563–587.

[32] RILEM Draft Recommendation TC 50-FMC (1985) Determination of the fracture energy of mortar and concrete by means of three-point bend test on notched beams. *Materials & Structures*, 18, 285–290.

[33] RILEM Draft Recommendation TC 89-FMT (1990a) Determination of the fracture parameters K_{Ic}^{S} a $CTOD_{\mathrm{c}}$ of plain concrete using three-point bend tests. *Materials & Structures*, 23, 457–460.

[34] Shah, S.P., Swartz, S.E. Ouyang, C. (1995) *Fracture mechanics of structural concrete: applications of fracture mechanics to concrete, rock, and other quasi-brittle materials*. John Wiley & Sons, Inc., New York.

[35] Sousa, R.A., Castro, J.T.P., Lopes, A.A.O., Martha, L.F. (2012) On improved crack tip plastic zone estimates based on T-stress and on complete stress fields. *Fatigue & Fracture Engineering Materials & Structures*, 36, 25–38.

[36] Tada, H., Paris, P.C., Irwin, G.R. (2000) *The stress analysis of cracks handbook* (3rd edition). Professional Engineering Publishing, Ltd., Bury St. Edmunds, UK.

[37] van Mier, J.G.M. (1997) *Fracture processes of concrete: Assessment of material parameters for fracture models*. CRC Press, Boca Raton.

[38] van Mier, J.G.M., van Vliet, M.R.A. (2002) Uniaxial tension test for determination of fracture parameters of concrete: state of the art. *Engineering Fracture Mechanics*, 69, 235–247.

[39] Vidya Sagar, R., Raghu Prasad, B.K. (2009a) AE energy release during the fracture of HSC beams. *Magazine of Concrete Research*, 61(6), 419–435.

[40] Vidya Sagar, R., Raghu Prasad, B.K., Karihaloo, B.L. (2010) Verification of the applicability of lattice model to concrete fracture by AE study. *International Journal of Fracture*, 161, 121–129.

[41] Wallin, K. (2013) A simple fracture mechanical interpretation of size effects in concrete fracture toughness tests. *Engineering Fracture Mechanics*, 99, 18–29.

[42] Wendner, R., Vorel, J., Smith, J., Hoover, Ch.G., Bažant, Z.P., Cusatis, G. (2014) Characterization of concrete failure behavior: a comprehensive experimental database for the calibration and validation of concrete models. *Materials & Structures*. doi:10.1617/s11527-014-0426-04.

[43] Williams, M. L. (1957) On the stress distribution at the base of stationary crack. *Journal of Applied Mechanics (ASME)*, 24, 109–114.

[44] Xu, S., Reinhardt, H.W. (1999a) Determination of double-K criterion for crack propagation in quasi-brittle fracture, Part I: Experimental investigation of crack propagation. *International Journal of Fracture*, 98(2), 111–149.

[45] Xu, S., Reinhardt, H.W. (1999b) Determination of double-K criterion for crack propagation in quasi-brittle fracture, Part II: Analytical evaluating and practical measuring methods for three-point bending notched beams. *International Journal of Fracture*, 98(2), 151–177.

References to relevant author's works

[46] Frantík, P., Veselý, V., Keršner, Z. (2013) Parallelization of lattice modelling for estimation of fracture process zone extent in cementitious composites. *Advances in Engineering Software*, 60–61, 48–57. doi: 10.1016/j.advengsoft.2012.11.020.

[47] Klon, J., Veselý, V. (2016) Energy dissipation during quasi-brittle fracture associated with the crack and the fracture process zone progression. Submitted to conference *Fracture and Damage Mechanics*, Budva, Montenegro, 2015. Accepted to *Key Engineering Materials*, expected in 2016.

[48] Seitl, S., Korte, S., De Corte, W., Boel, V., Sobek, J., Veselý, V. (2014) Selecting a suitable specimen shape with low constraint value for determination of fracture param-

eters of cementitious composites. *Key Engineering Materials*, Vols. 577–578, 481–484. doi:10.4028/www.scientific.net/KEM.577-578.481.

[49] Sobek, J., Veselý, V., Seitl, S. (2014) Combination of wedge splitting and bending fracture test – crack tip stress field and nonlinear zone extent analysis. *Avanced Material Research*, 969, 67–72. doi:10.4028/www.scientific.net/AMR.969.67.

[50] Vavřík, D., Jandejsek, I., Fíla, T., Veselý, V. (2013) Radiographic observation and semi-analytical reconstruction of fracture process zone in silicate composite specimen. *Acta Technica*, 58, 315–326. ISSN 0001-7043.

[51] Veselý, V., Frantík, P. (2010) Reconstruction of fracture process zone during tensile failure of quasi-brittle materials. *Applied and Computational Mechanics*, 4, 237–250. ISSN 1802-680X.

[52] Veselý, V., Frantík, P. (2014) An application for the fracture characterisation of quasi-brittle materials taking into account fracture process zone influence. *Advances in Engineering Software*, 72, 66–76. doi: 10.1016/j.advengsoft.2013.06.004.

[53] Veselý, V., Frantík, P., Keršner, Z. (2009) Cracked volume specified work of fracture. In: Proc. of the *12th Int. Conf. on Civil, Structural and Environmental Engineering Computing*, B.H.V. Topping, L.F. Costa Neves and R.C. Barros (eds.), Funchal, Portugal, 2009. Civil-Comp Press, Stirlingshire, United Kingdom, paper 194, 18 p. doi:10.4203/ccp.91.194.

[54] Veselý, V., Frantík, P., Sobek, J., Malíková, L., Seitl, S. (2015a) Multi-parameter crack tip stress state description for evaluation of nonlinear zone width in silicate composite specimens in component splitting/bending test geometry. *Fatigue & Fracture of Engineering Materials & Structures* (Special Issue: Characterisation of crack tip fields), 38(2), 200–214. doi:10.1111/ffe.12170.

[55] Veselý, V., Frantík, P., Vidya Sagar, R., Štafa, M., Pail, T. (2014) Balanced energy dissipation at propagating crack tip in quasi-brittle materials? – Analysis via soft-computing methods. *Key Engineering Materials*, Vols. 577–578, 269–272. doi:10.4028/www.scientific.net/KEM.577-578.269.

[56] Veselý, V., Keršner, Z., Němeček, J., Frantík, P., Řoutil, L., Kucharczyková, B. (2010) Estimation of fracture process zone extent in cementitious composites. *Chem. Listy*, 104, s382–s385. ISSN 0009-2770.

[57] Veselý, V., Řoutil, L., Keršner, Z. (2007c) Structural geometry, fracture process zone and fracture energy. In: Proc. of *Fracture Mechanics of Concrete and Concrete Structures (FraMCoS-6)*, Al. Carpinteri, P. Gambarova, G. Ferro, G. Plizzari (eds.), Catania, Italy, 2007. Taylor & Francis/Balkema, vol. 1, 111–118. ISBN 978-0-415-44065-3.

[58] Veselý, V., Sobek, J. (2013) Numerical study of failure of cementitious composite specimens in modified compact tension fracture test. *Transactions of the VŠB–Technical University of Ostrava*, 2(13), Civil Engineering Series, 180-–187. doi:10.2478/tvsb-2013-0025.

[59] Veselý, V., Sobek, J., Šestáková, L., Frantík, P., Seitl, S. (2013a) Multi-parameter crack tip stress state description for estimation of fracture process zone extent in silicate composite WST specimens. *Frattura ed Integrità Strutturale* (Special Issue: Characterization of Crack Tip Stress Field), 25, 69–78. Gruppo Italiano Frattura, Italia. doi:10.3221/IGF-ESIS.25.11.

Summary in Czech

Tahové porušování kvazikřehkých materiálů je spojeno se vznikem a vývojem tzv. lomové procesní zóny (LPZ) na čele šířící se trhliny. Pro ověření přístupů jak numerického modelování kvazikřehkého chování, tak experimentálního určení odpovídajících lomových parametrů si nevystačíme pouze s informací o existenci této oblasti porušování materiálu, ale potřebujeme znát také parametry, kterými lze tato zóna popsat (objem, tvar a rozložení disipace energie).

Práce představuje Java aplikaci vytvořenou pro pokročilé určení lomových charakteristik materiálů na silikátové bázi porušující se kvazikřehkým způsobem. Tento nástroj provádí rekonstrukci průběhu kvazikřehkého lomu z naměřené křivky zatížení vs. posun a znalosti základních mechanických vlastností materiálu, z čehož plyne i název této aplikace (jde o akronym anglického názvu *Re*construction of *Frac*ture *Pro*cess – ReFraPro). Hlavním přínosem navržené metodologie je to, že bere do úvahy charakteristiky LPZ, konkrétně její velikost a tvar, a zavádí je do procedur pro určení lomových parametrů. Očekává se, že tento přístup výrazně sníží vliv velikosti/tvaru zkušebního tělesa na hodnoty parametrů nelineárních lomových modelů určovaných ze záznamů lomových testů na laboratorních tělesech. Do této aplikace je implementována vyvinutá technika pro odhad velikosti a tvaru LPZ. Tato technika je založena na kombinaci několika přístupů a teorií aplikovatelných v oblasti porušování konstrukčních materiálů, tj. multiparametrové lomové mechaniky, klasických nelineárních lomových modelů pro beton (modely ekvivalentní elastické trhliny a modely kohezivní trhliny) a teorie plasticity. Znalost rozsahu LPZ je v rámci tohoto přístupu využita pro vztažení části celkové hodnoty lomové práce právě k charakteristikám LPZ.

Práce je dále zaměřena na verifikaci a validaci vyvíjené metody ReFraPro. Pro tento účel posloužily výsledky z měření akustické emise vybrané z literatury a výsledky vlastních provedených testů doprovázených prozařováním tělesa pomocí rentgenového paprsku. Některé sady publikovaných dat nemají pro důkladnou validaci metody ReFraPro dostatečný rozsah. Byly tedy provedeny numerické simulace sloužící k doplnění informací potřebných pro ověření této techniky. Bylo dosaženo dobré shody mezi rozsahy LPZ predikovanými metodou ReFraPro a výsledky simulací, i vybranými experimentálními daty.

Dále byla pozornost zaměřena na numerické studie nových geometrií pro lomové zkoušky kvazikřehkých materiálů, které poskytnou široký rozsah podmínek stísnění napětí a deformace u čela trhliny, což ovlivní lomovou procesní zónu, tj. objem, kde dochází k zásadním procesům rozhodujícím o šíření porušení a jeho rozsahu (včetně odpovídající disipace energie).

Poslední část předkládané práce je zacílena na aproximaci polí napětí a deformací jak v bezprostřední blízkosti čela trhliny, tak také v jejím vzdálenějším okolí, a to v tělesech používaných pro určování lomových charakteristik kvazikřehkých materiálů. Hodnoty koeficientů členů vyšších řádů Williamsovy mocninné řady jsou určeny z výsledků výpočtů metodou konečných prvků a následně použity pro analytickou aproximaci (zpětnou rekonstrukci) pole napětí v tělese s trhlinou. Je diskutována shoda mezi analytickým a numerickým řešením, jež závisí na vzdálenosti od kořene trhliny a počtu členů řady.